

From Sequences to Structures and Back

The Vienna RNA Package

Peter Schuster

Institut für Theoretische Chemie, Universität Wien, Austria

and

The Santa Fe Institute, Santa Fe, New Mexico, USA

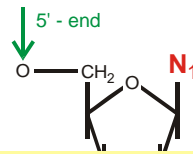


Siemens PSE Life Science Symposium

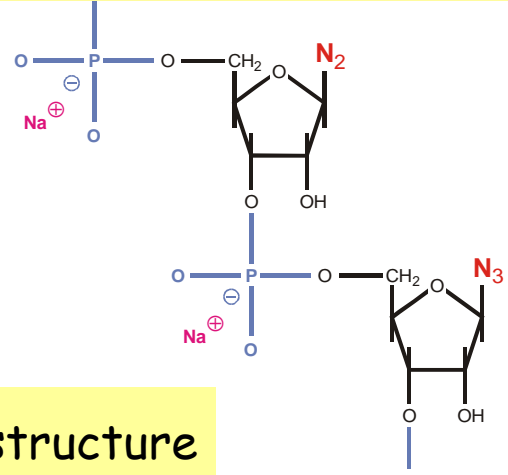
Brno, 14.03.2006

Web-Page for further information:

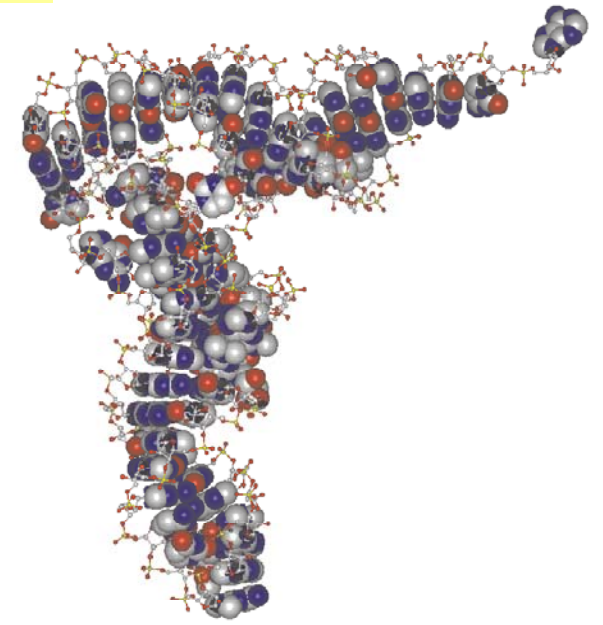
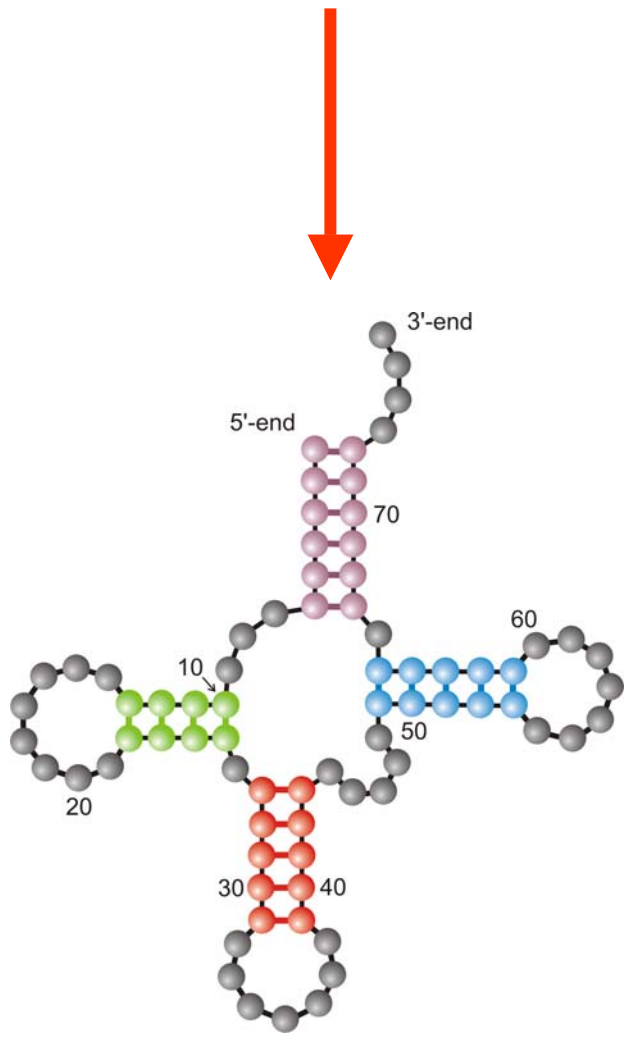
<http://www.tbi.univie.ac.at/~pks>

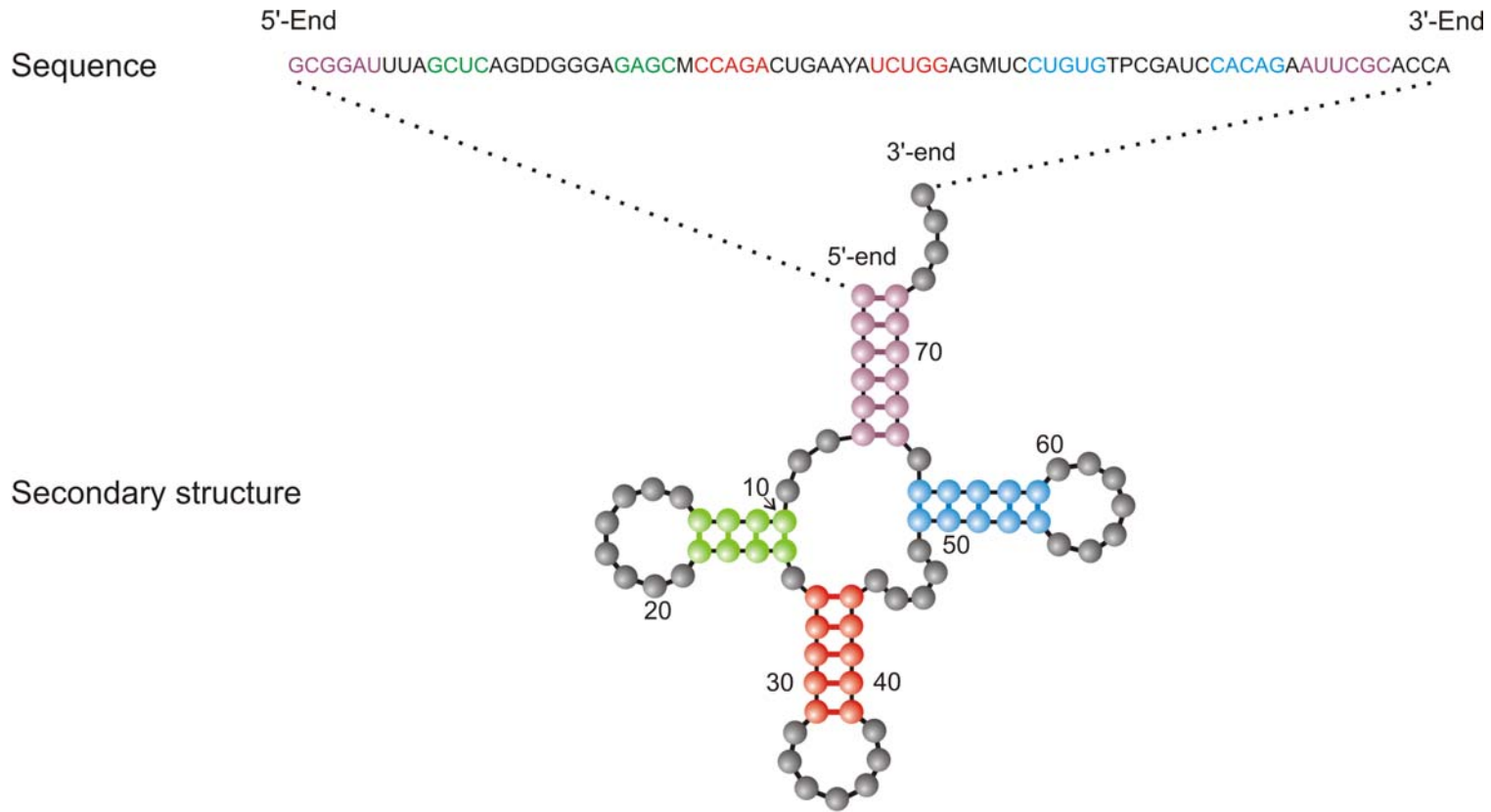


5'-end **GCGGAUUUAGCUC**AGUUGGGAGAG**CGCCAGACUGAAGAUCUGG**AGGUC**CUGUGUUCGAUCCACAGAAUUCGCACCA** 3'-end

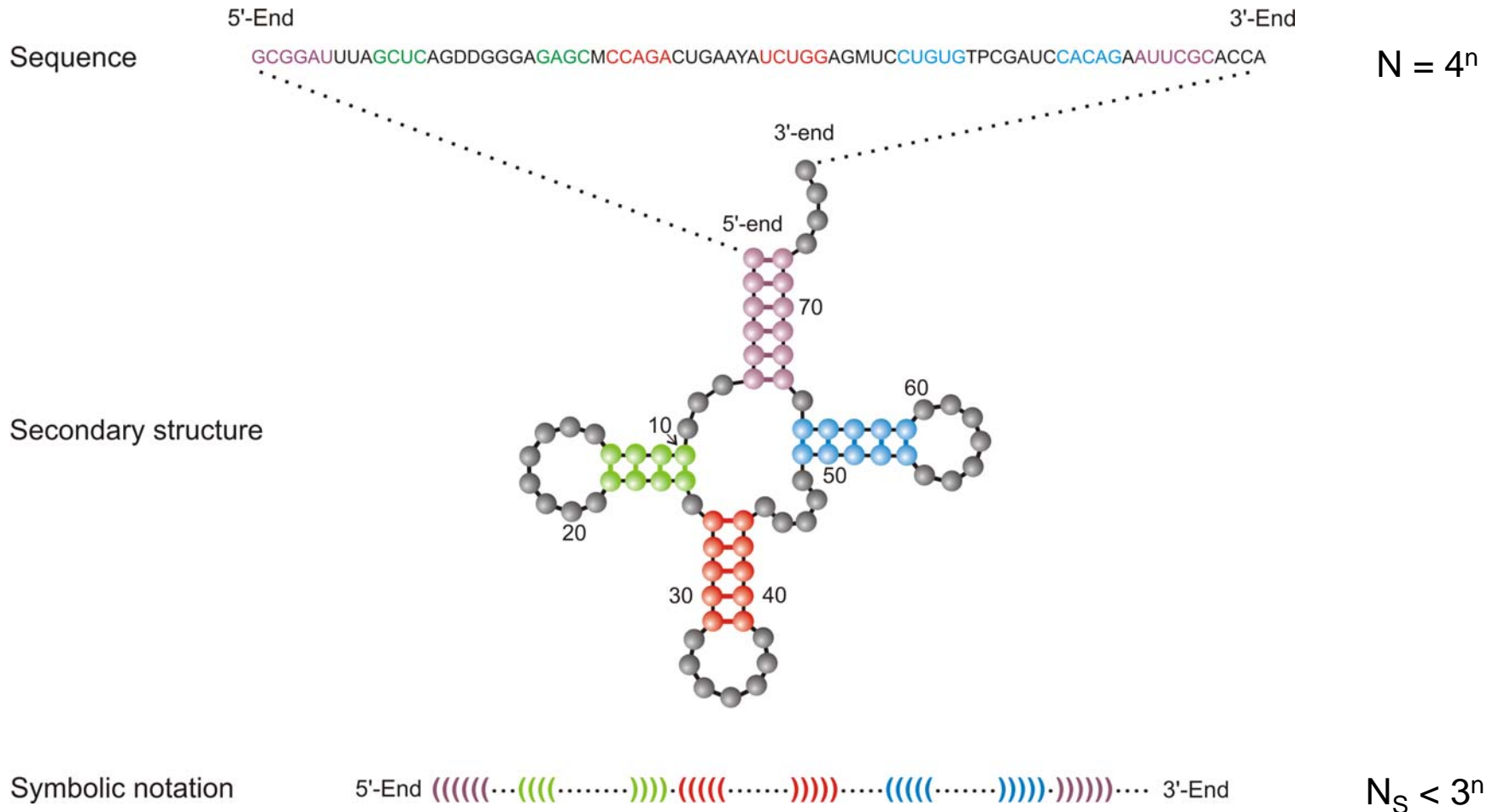


Definition of RNA structure





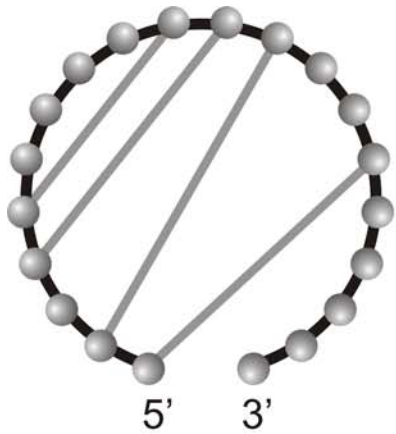
A symbolic notation of RNA secondary structure that is equivalent to the conventional graphs



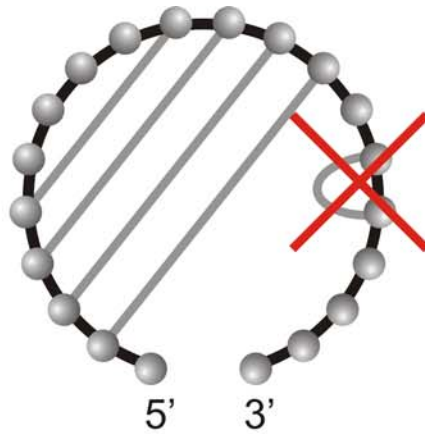
Criterion: Minimum free energy (mfe)

Rules: $_ (_) _ \in \{AU, CG, GC, GU, UA, UG\}$

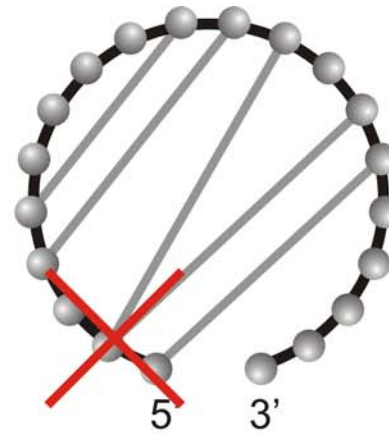
A symbolic notation of RNA secondary structure that is equivalent to the conventional graphs



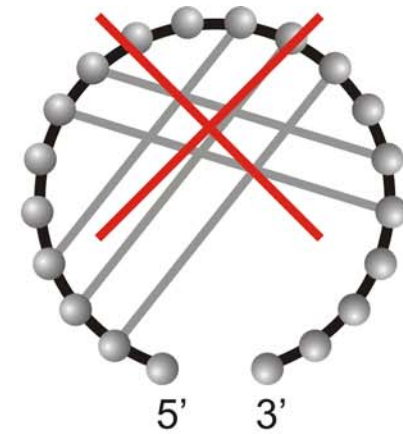
Base pairing



No nearest neighbor pair rule



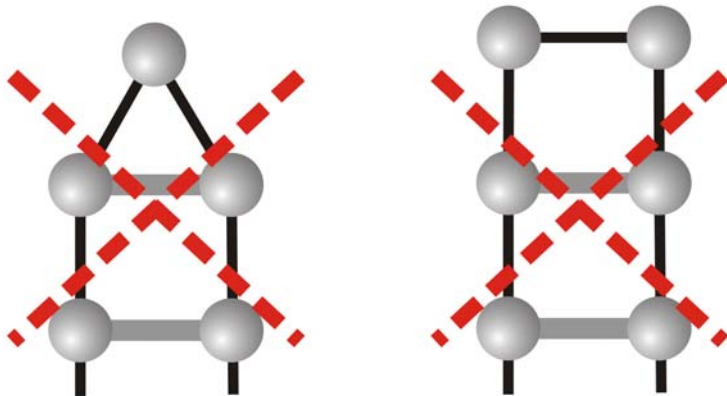
No base triplet rule



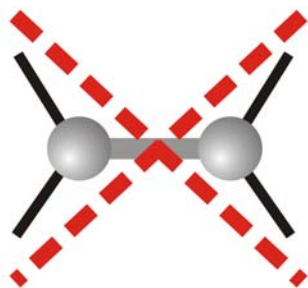
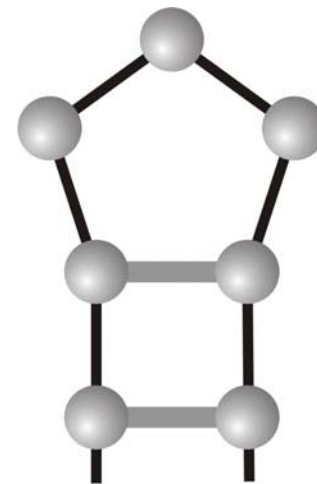
No pseudoknot rule

Base pairs $\in \{\mathbf{AU}, \mathbf{CG}, \mathbf{GC}, \mathbf{GU}, \mathbf{UA}, \mathbf{UG}\}$

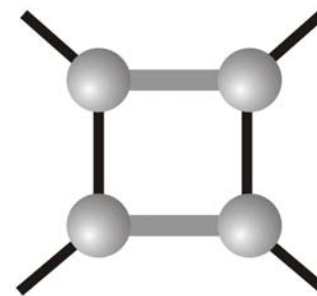
Conventional definition of RNA secondary structures



Impossible (extremely high free energies)
for steric reasons



High free energies because of lack of stacking and
very rare in minimum free energy structures



Restrictions on physically acceptable mfe-structures: $\lambda \geq 3$ and $\sigma \geq 2$

Vienna RNA Package

RNAfold

RNAdistance

RNAinverse

RNAduplex

RNAsubopt

RNAeval

RNAcofold

RNAheat

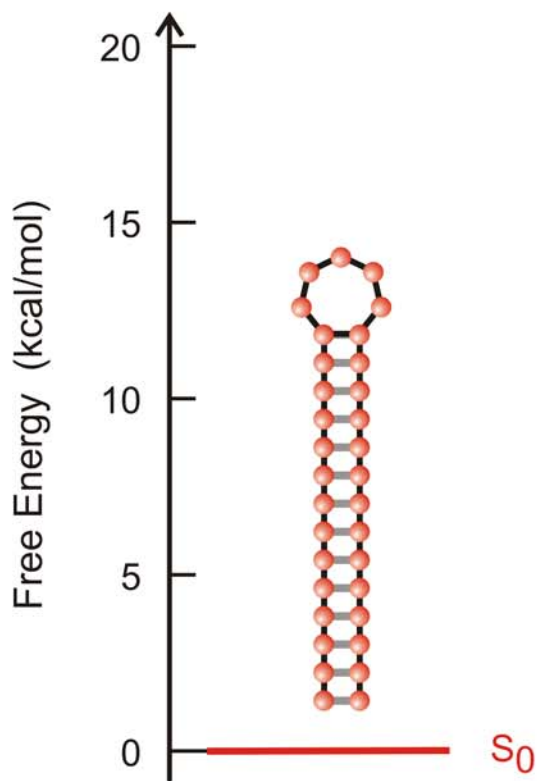
RNApdist

RNAalifold

RNAplot

<http://www.tbi.univie.ac.at/RNA/>

One sequence - one structure



Minimum free energy structure

RNA sequence

GUAUCGAAAUACGUAGCGUAUGGGGAUGCUGGACGGUCCCAUCGGUACUCCA

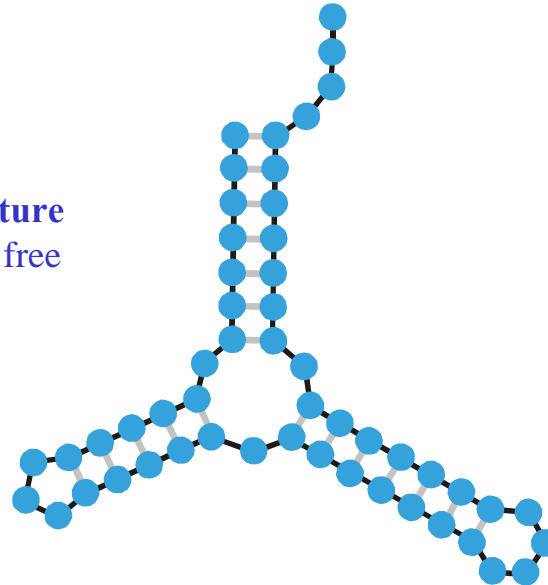
RNA folding:
Structural biology,
spectroscopy of
biomolecules,
understanding
molecular function

Biophysical chemistry:
thermodynamics and
kinetics



Empirical parameters

RNA structure
of minimal free
energy

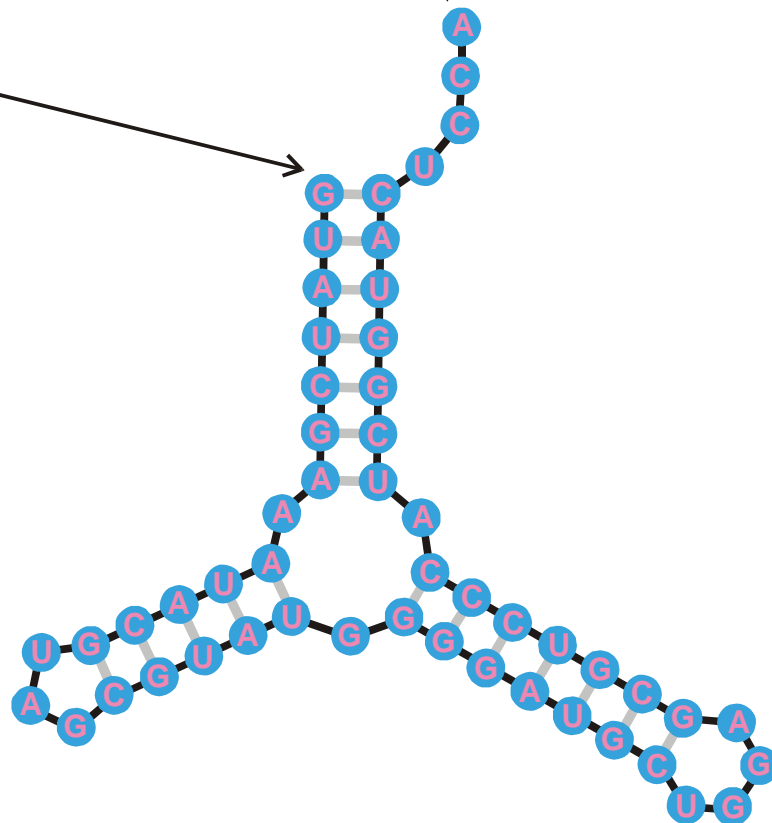
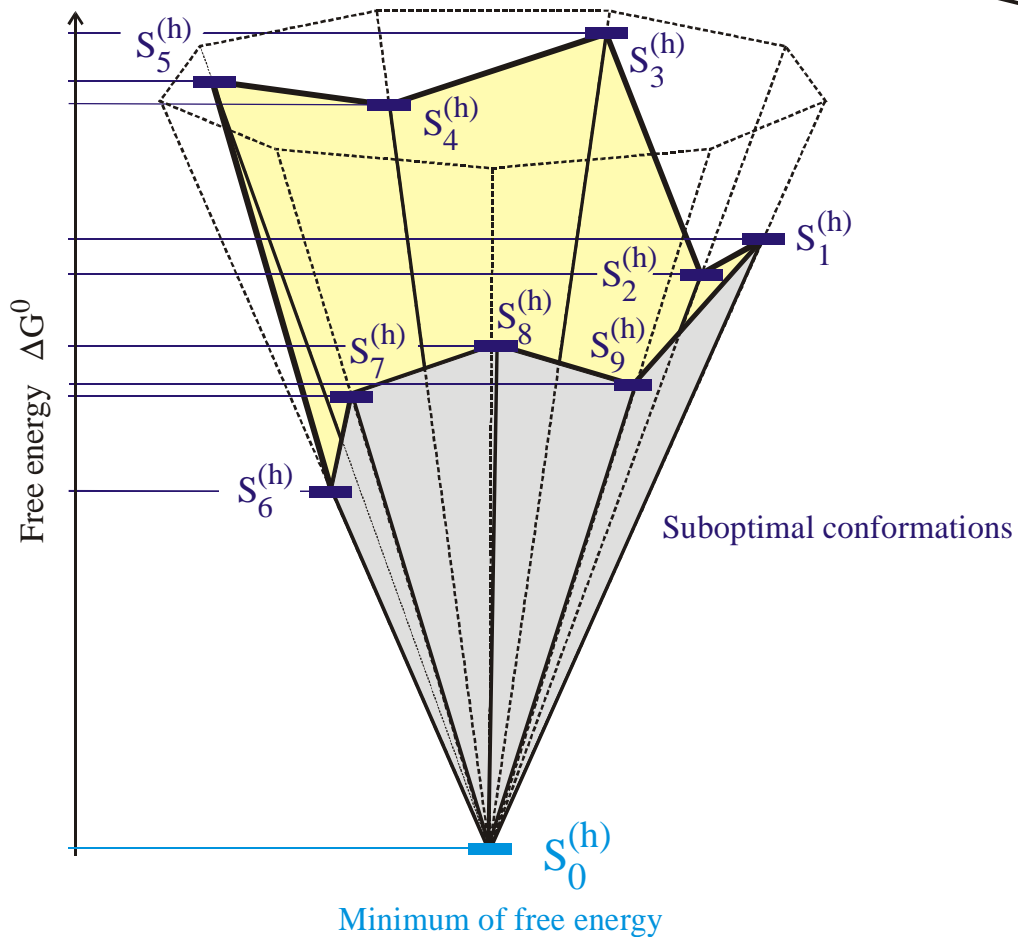


Sequence, structure, and design

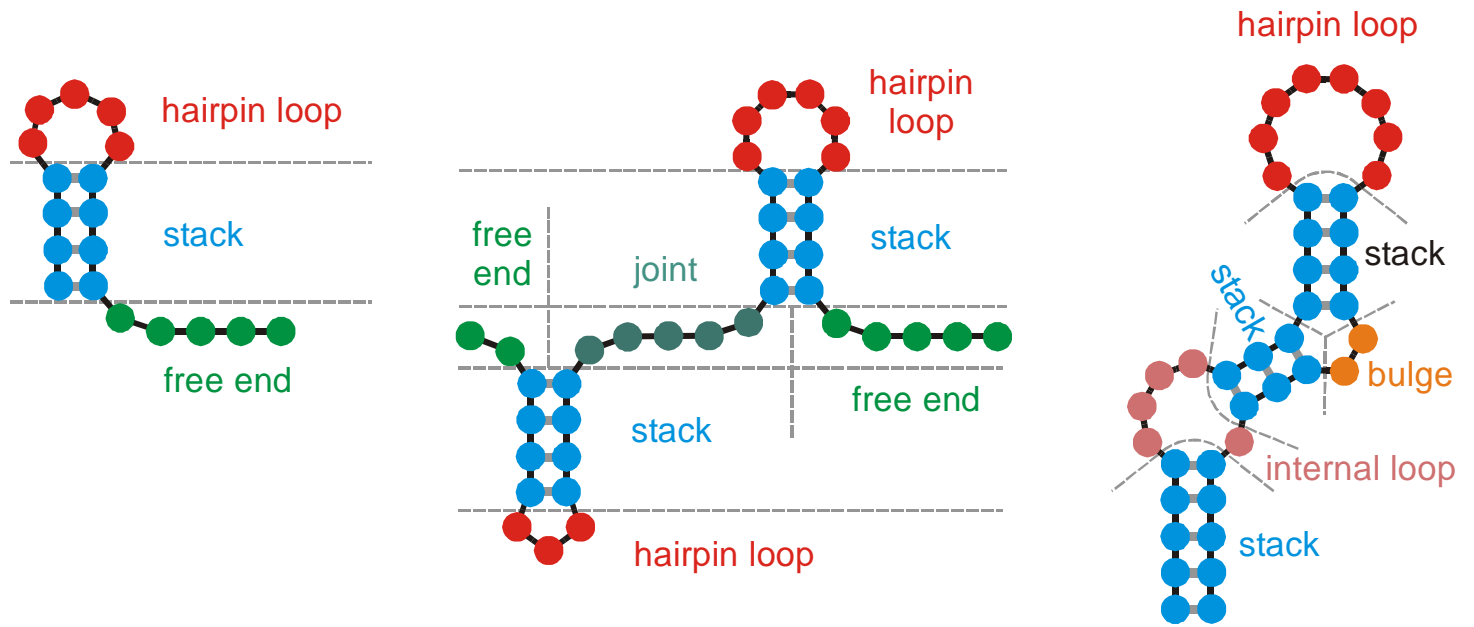
5'-end

3'-end

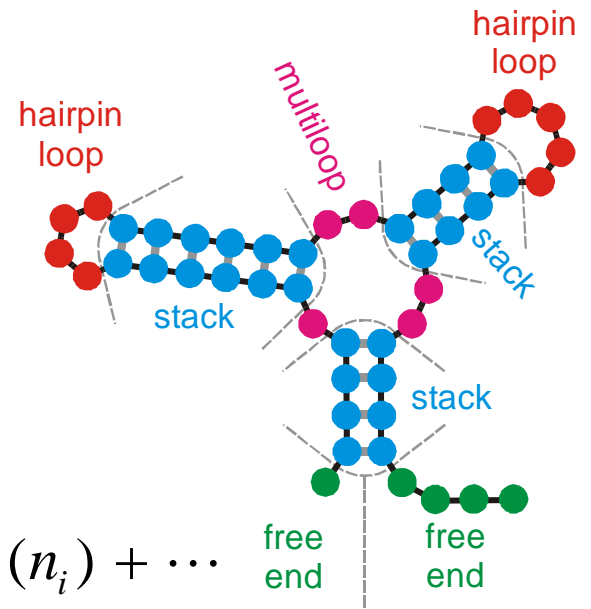
GUAUCGAAUACGUAGCGUAUGGGGAUGCUGGACGGUCCCAUCGGUACUCCA



The minimum free energy structures on a discrete space of conformations



Elements of RNA
secondary structures
as used in free energy
calculations



$$\Delta G_0^{300} = \sum_{\text{stacks of base pairs}} g_{ij,kl} + \sum_{\text{hairpin loops}} h(n_l) + \sum_{\text{bulges}} b(n_b) + \sum_{\text{internal loops}} i(n_i) + \dots$$

RNA sequence

GUAUCGAAAUACGUAGCGUAUGGGGAUGCUGGACGGUCCCAUCGGUACUCCA

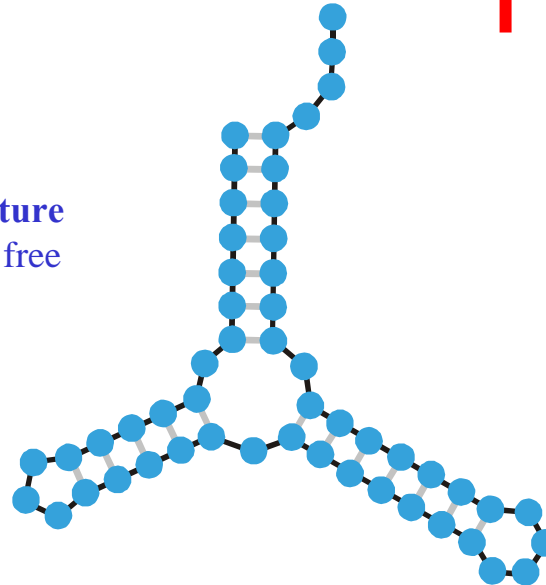
RNA folding:
Structural biology,
spectroscopy of
biomolecules,
understanding
molecular function

Iterative determination
of a sequence for the
given secondary
structure

**Inverse Folding
Algorithm**

Inverse folding of RNA:
Biotechnology,
design of biomolecules
with predefined
structures and functions

RNA structure
of minimal free
energy



Sequence, structure, and design

Inverse folding algorithm

$I_0 \rightarrow I_1 \rightarrow I_2 \rightarrow I_3 \rightarrow I_4 \rightarrow \dots \rightarrow I_k \rightarrow I_{k+1} \rightarrow \dots \rightarrow I_t$

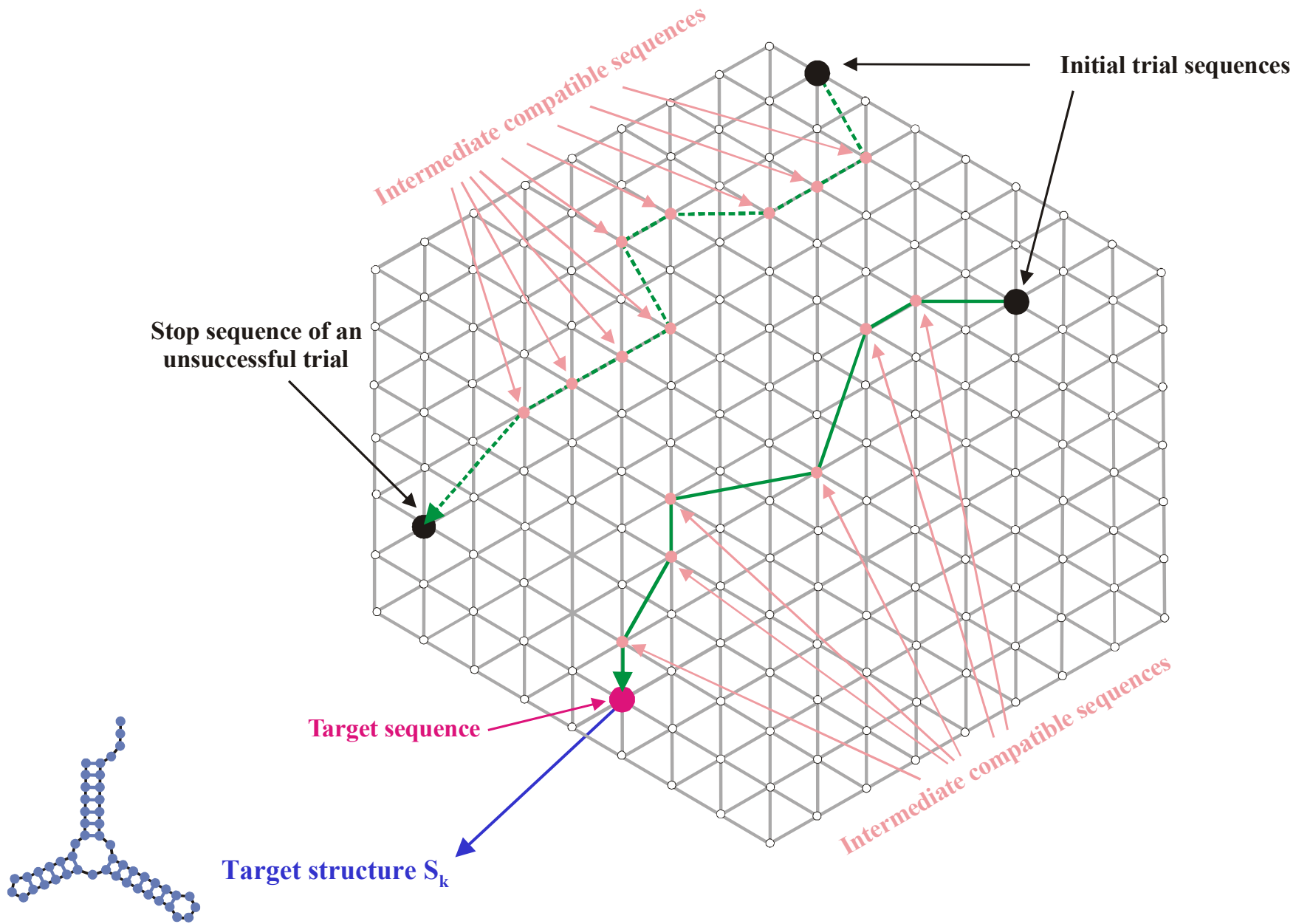
$S_0 \rightarrow S_1 \rightarrow S_2 \rightarrow S_3 \rightarrow S_4 \rightarrow \dots \rightarrow S_k \rightarrow S_{k+1} \rightarrow \dots \rightarrow S_t$

$$I_{k+1} = \mathfrak{M}_k(I_k) \quad \text{and} \quad \Delta d_S(S_k, S_{k+1}) = d_S(S_{k+1}, S_t) - d_S(S_k, S_t) < 0$$

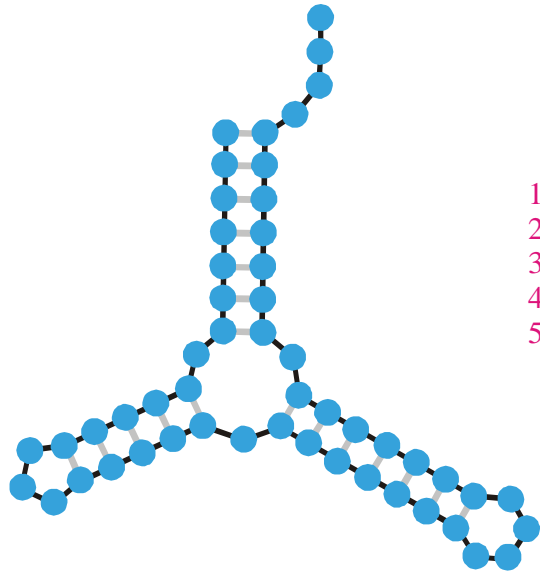
\mathfrak{M} ... base or base pair mutation operator

$d_S(S_i, S_j)$... distance between the two structures S_i and S_j

‘Unsuccessful trial’ ... termination after n steps



Approach to the **target structure S_k** in the inverse folding algorithm



Minimum free energy
criterion

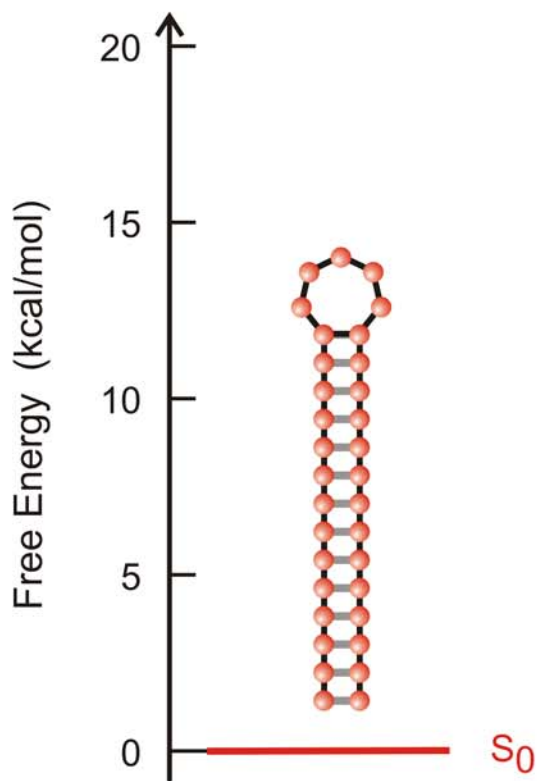
1st
2nd
3rd trial
4th
5th

→ GUAUCGAAAUACGUAGCGUAUGGGGAUGCUGGACGGUCCCAUCGGUACUCCA
 → UGGUUACGCGUUGGGGUAACGAAGAUUCCGAGAGGAGUUUAGUGACUAGAGG
 → CUUCUUGAGCUAGUACCUAGUCGGAUAGGAUUUCCUAUCUCCAGGGAGGAUG
 → CUUUUCUUCACGUUAGAUGUGUAAUGGACAUGUGUUUAAUUUAGGAAAGGCGC
 → AUAACGUGAGUGUCUAAUACUGAUCGCUCCGGAGGGUGGUGGCGUUGUAAU

Inverse folding of RNA secondary structures

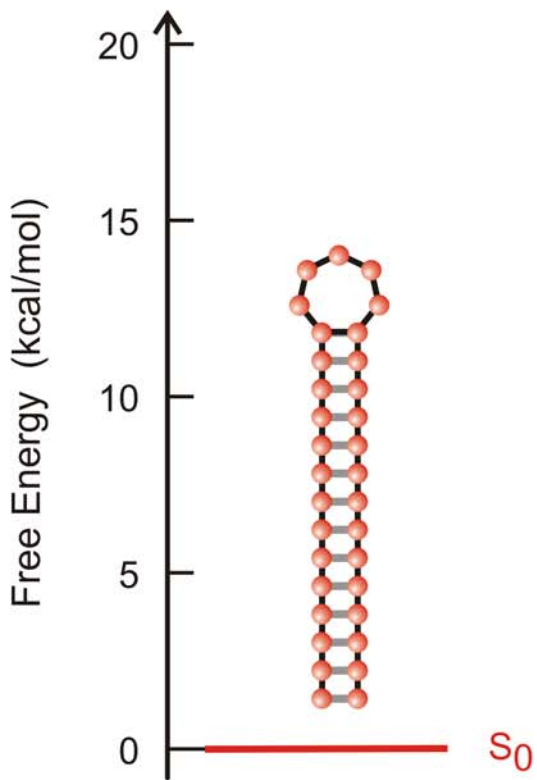
The inverse folding algorithm searches for sequences that form a given RNA secondary structure under the minimum free energy criterion.

One sequence - one structure



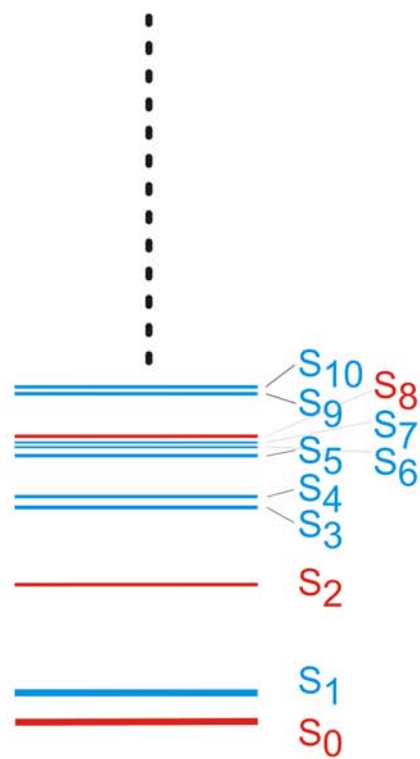
Minimum free energy structure

One sequence - one structure



Minimum free energy structure

Many suboptimal structures
Partition function

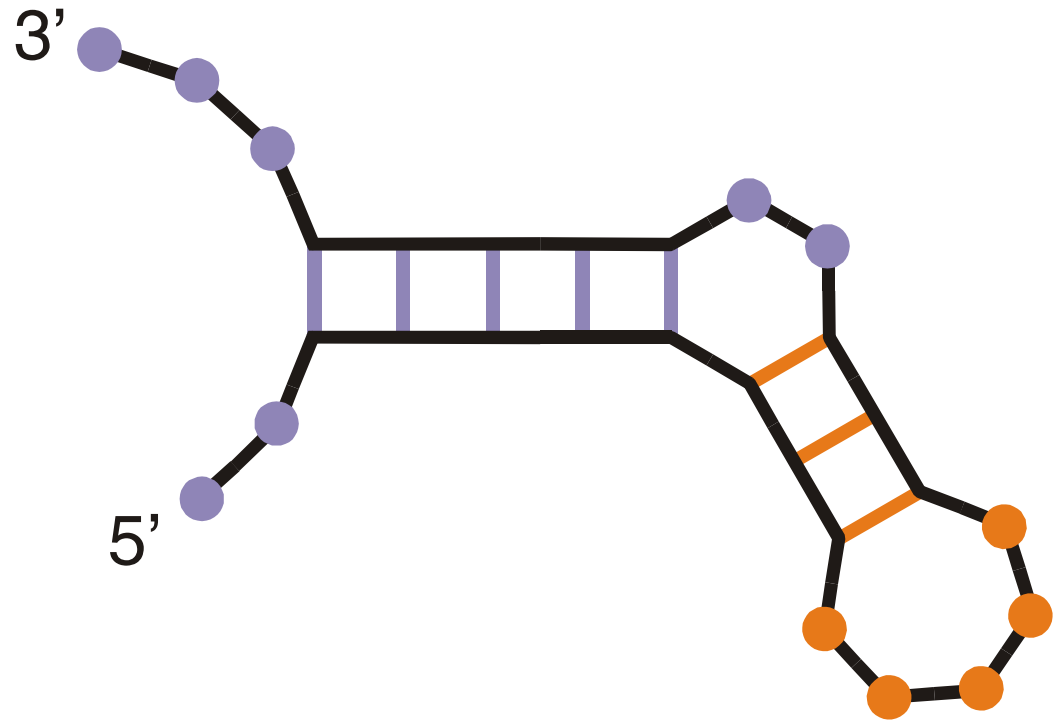


Suboptimal structures

base pair probability

$$p_{ij}(X, T) = \sum_k \gamma_k(T) a_{ij}(S_k) \quad \text{with} \quad \gamma_k(T) = g_k e^{-(\varepsilon_k - \varepsilon_0)/kT} / Q(T)$$
$$Q(T) = \sum_k \gamma_k(T)$$

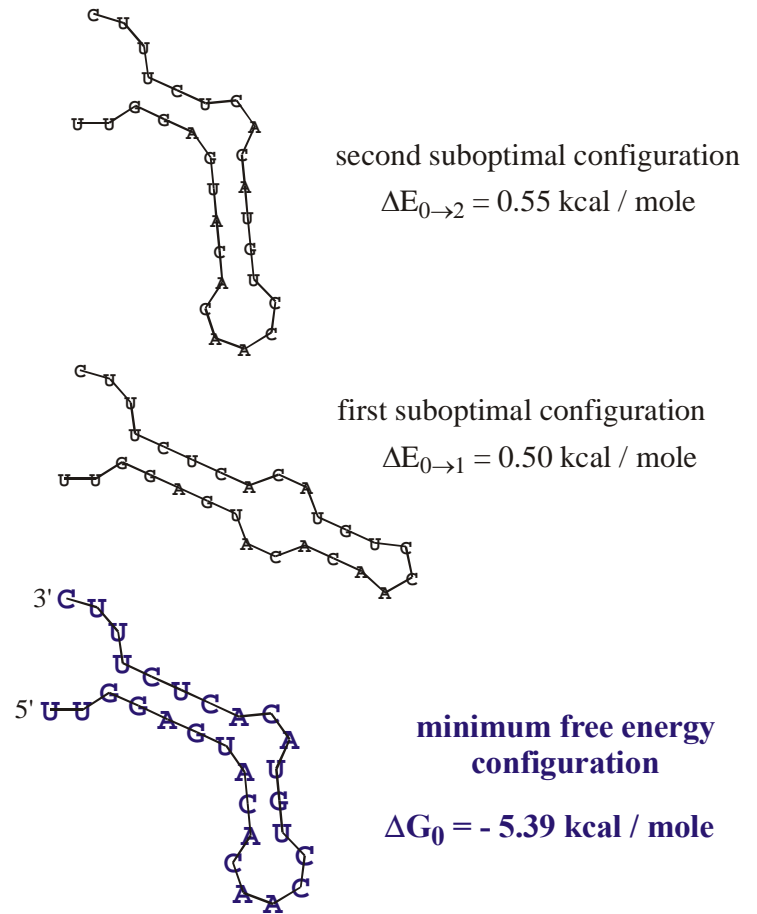
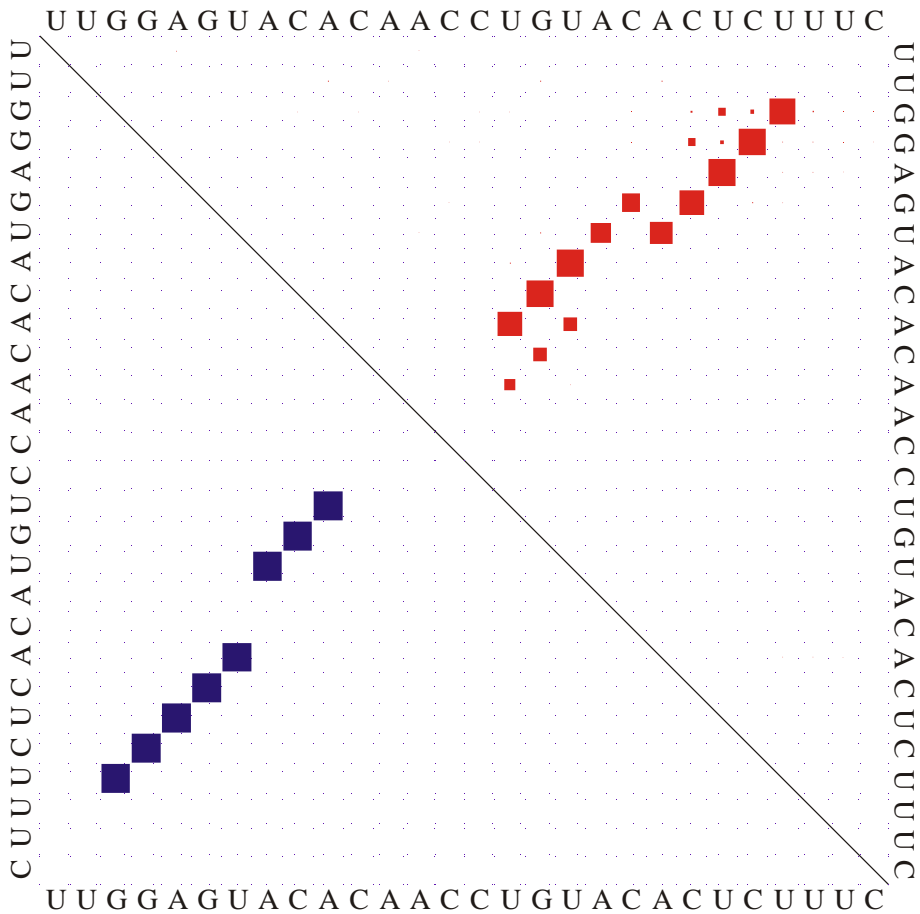
Base pair probability derived from the partition function $Q(T)$



UUGGAGUACACAACCGUACACUCUUUC

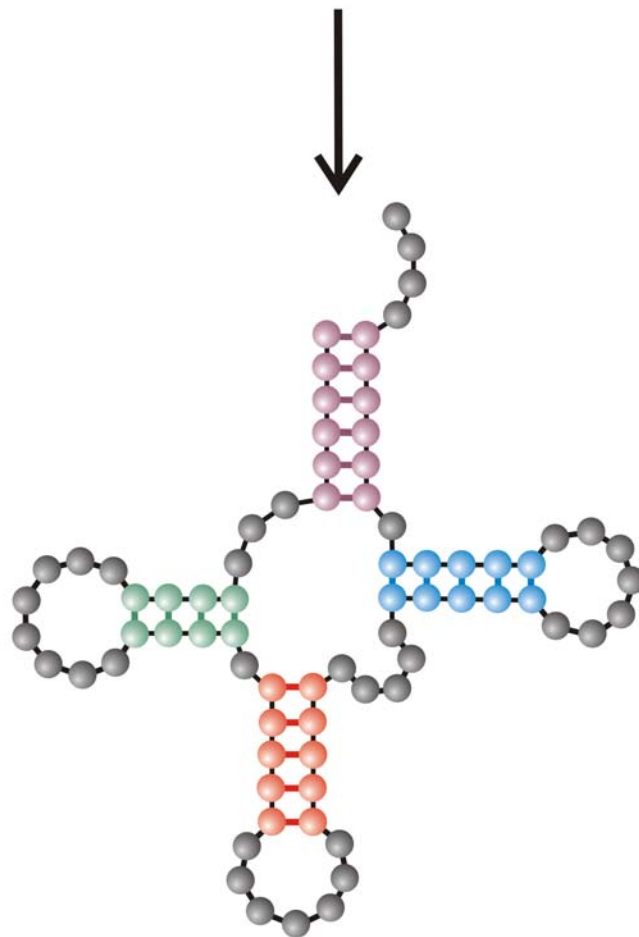
Example of a small RNA molecule with two low-lying suboptimal conformations which contribute substantially to the partition function

Example of a small RNA molecule: $n=28$

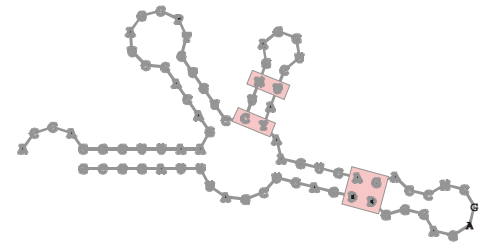
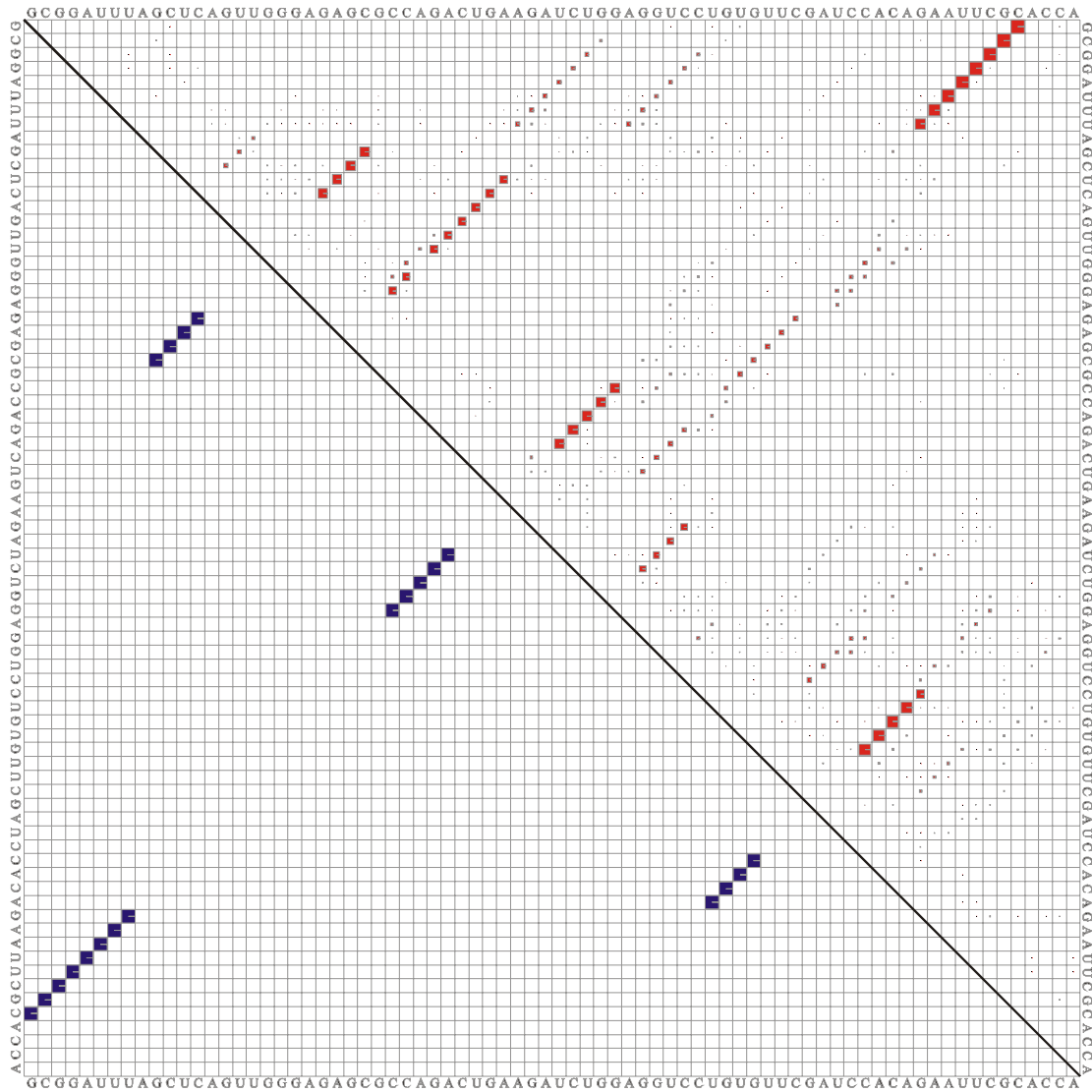


„Dot plot“ of the minimum free energy structure (**lower triangle**) and the partition function (**upper triangle**) of a small RNA molecule (n=28) with low energy suboptimal configurations

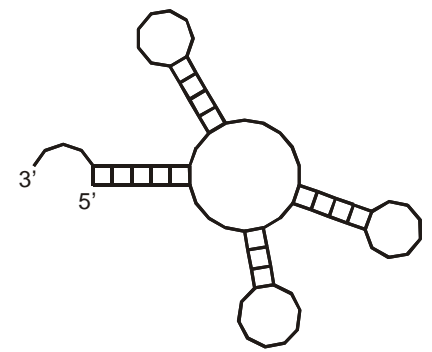
GCGGAUUUAGCUCAGUUGGGAGAGCGCCAGACUGAAGAUCUGGAGGUC CUGUGUUCGAUCCACAGAAUUCGCACCA
GCGGAUUUAGCUCAGDDGGGAGAGCMCCAGACUGAAYAUCUGGAGMUC CUGUGTPCGAUCCACAGAAUUCGCACCA



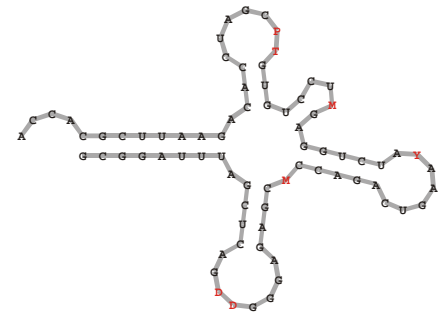
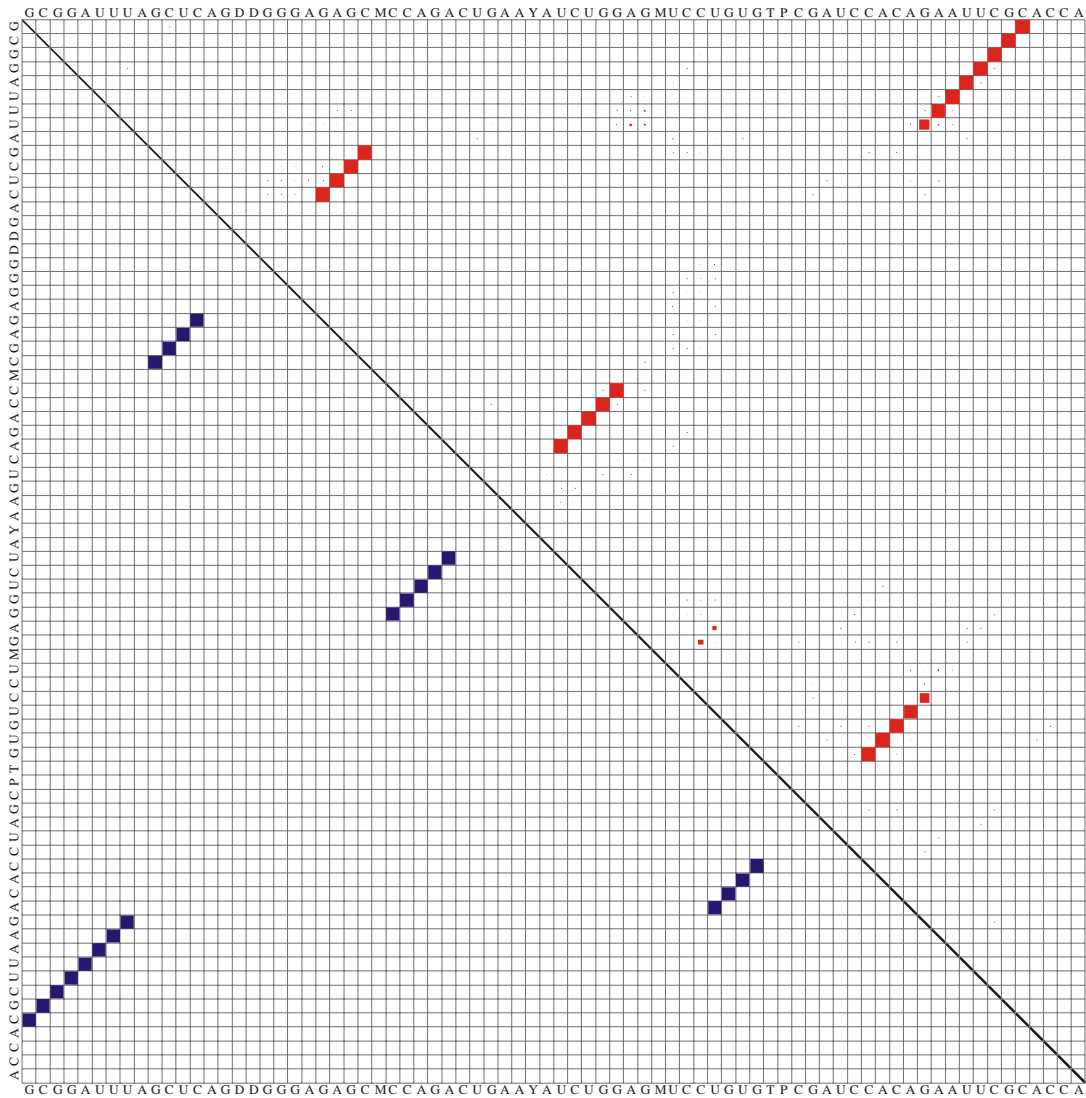
Phenylalanyl-tRNA as an example for the computation of the partition function



first suboptimal configuration
 $\Delta E_{0 \rightarrow 1} = 0.43 \text{ kcal / mole}$

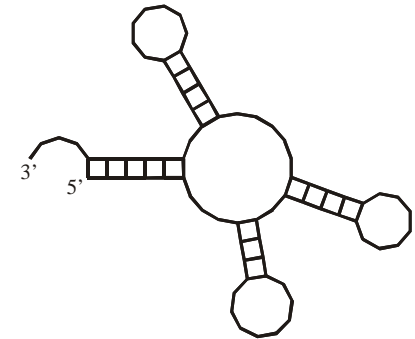


tRNA^{phe}
without modified bases



first suboptimal configuration

$$\Delta E_{0 \rightarrow 1} = 0.94 \text{ kcal / mole}$$



tRNA^{phe}

with modified bases

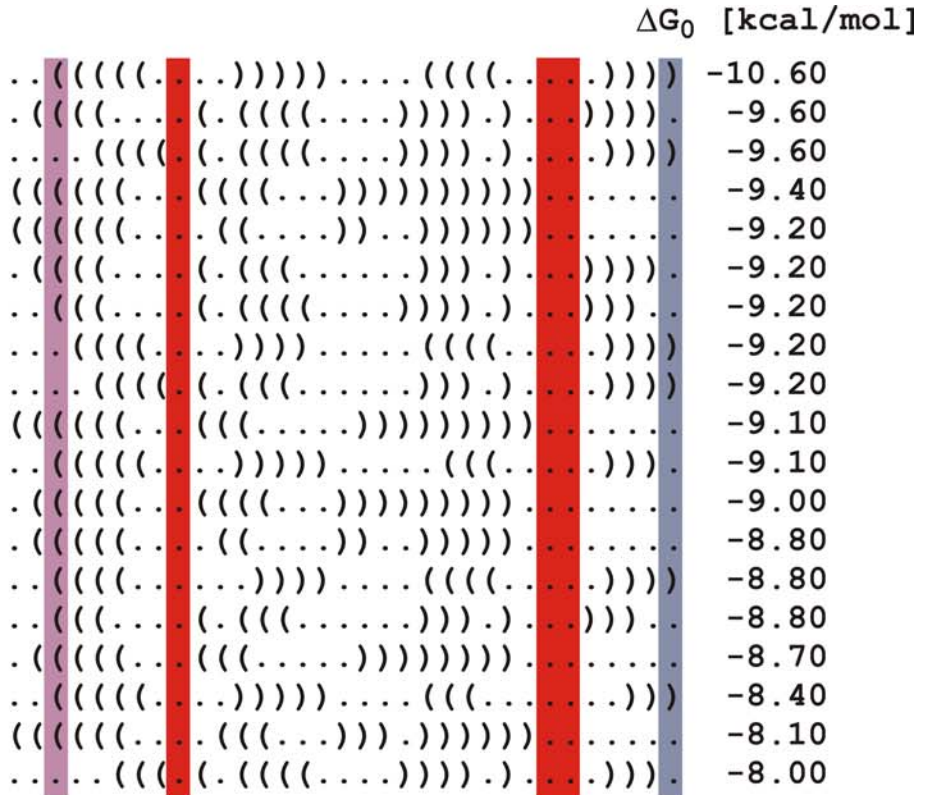
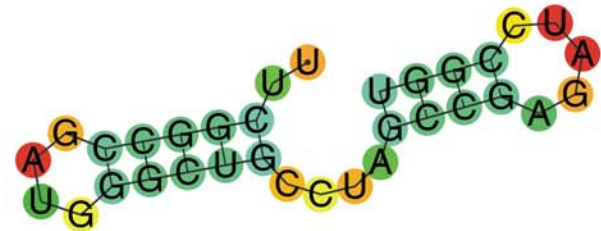
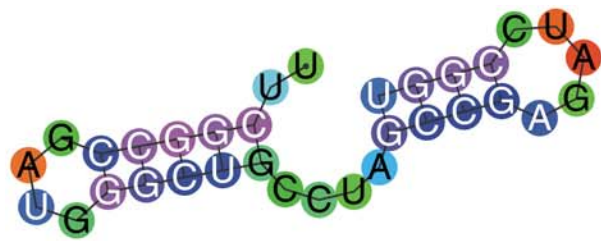
base pair probability

$$p_{ij}(X, T) = \sum_k \gamma_k(T) a_{ij}(S_k) \quad \text{with} \quad \gamma_k(T) = g_k e^{-(\varepsilon_k - \varepsilon_0)/kT} / Q(T)$$
$$Q(T) = \sum_k \gamma_k(T)$$

base pairing entropy

$$s_i = - \sum_j p_{ij} \ln p_{ij} \quad \text{with} \quad p_{ii} = 1 - \sum_{j, j \neq i} p_{ij}$$

Reliability measures for structure prediction



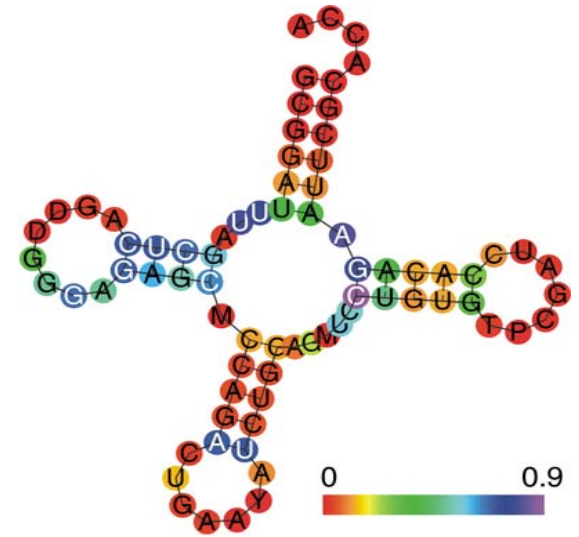
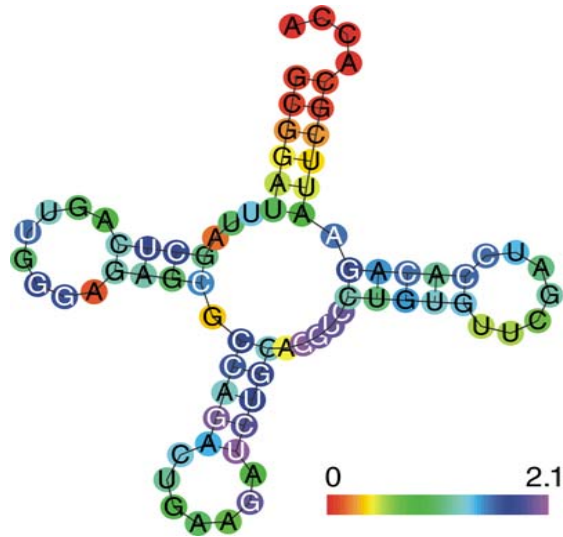
Base pairing entropy and base pair probability in a model RNA molecule

without modification

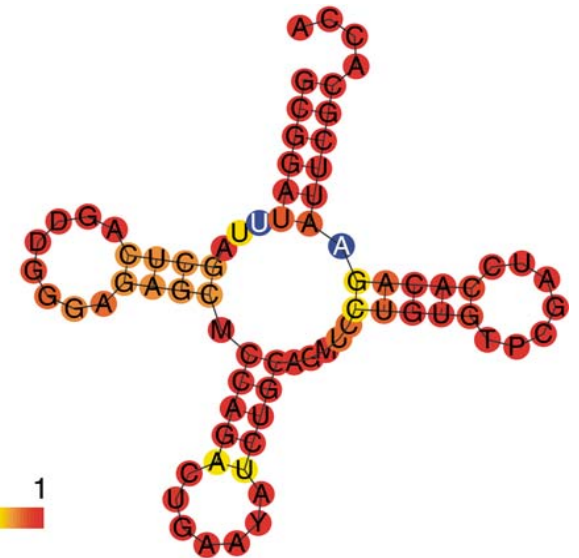
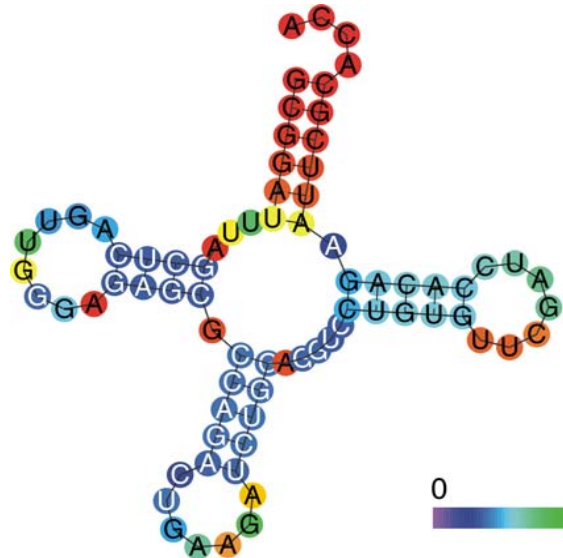
nucleotides

with modification

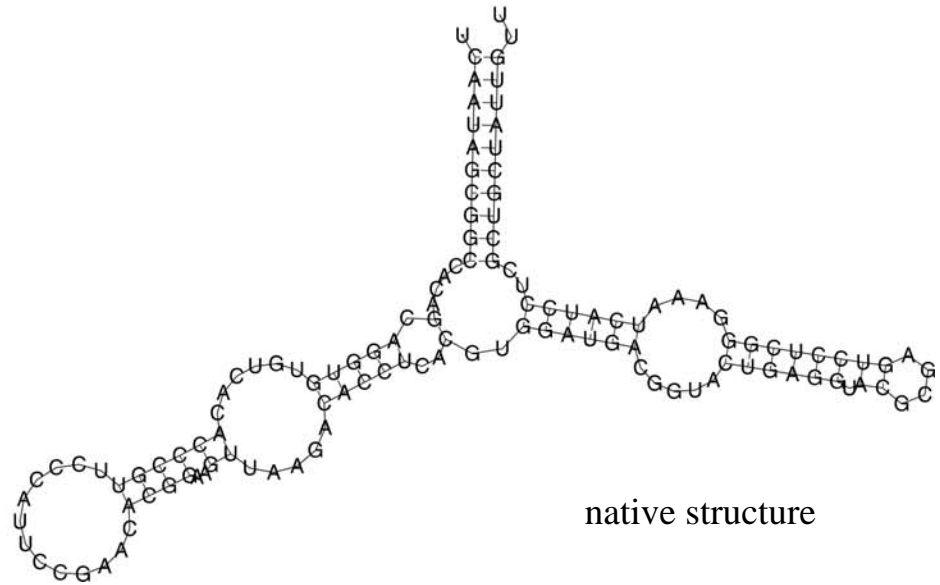
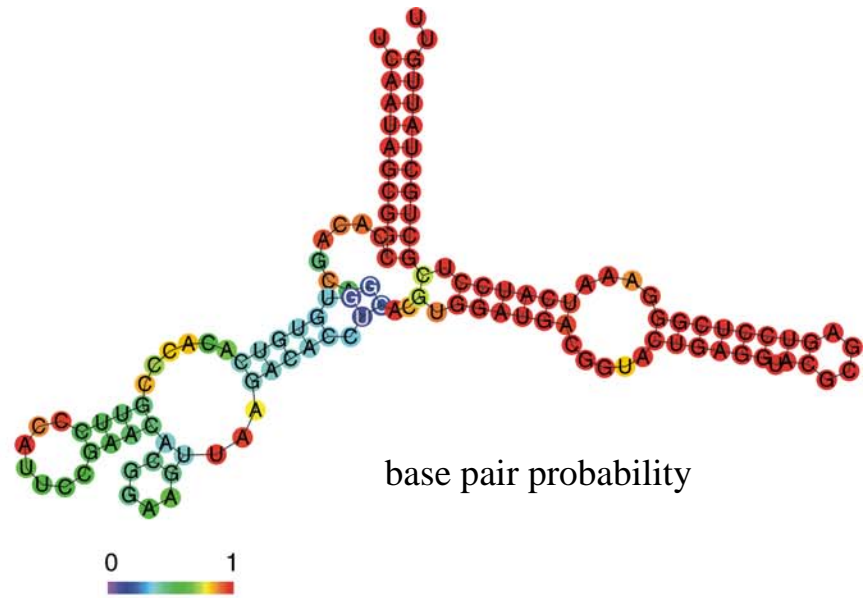
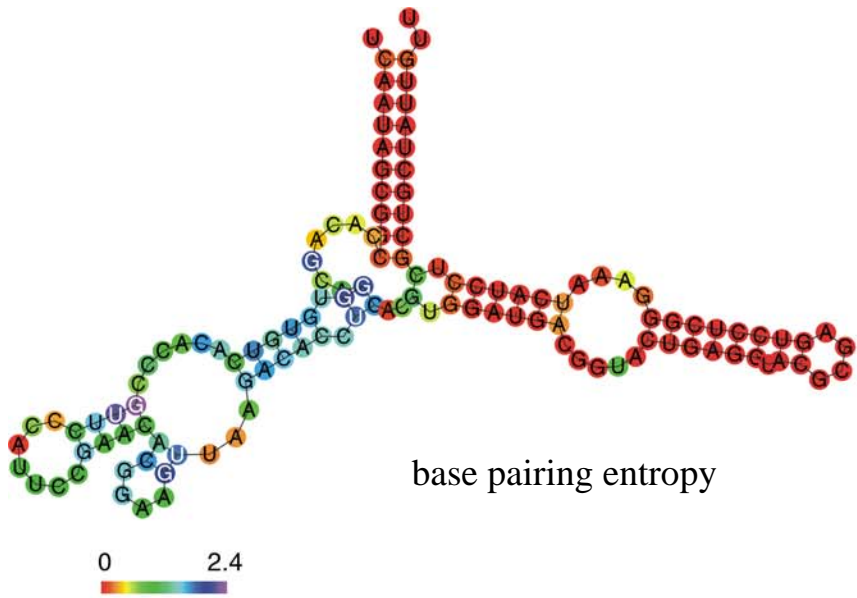
base pairing entropy



base pair probability

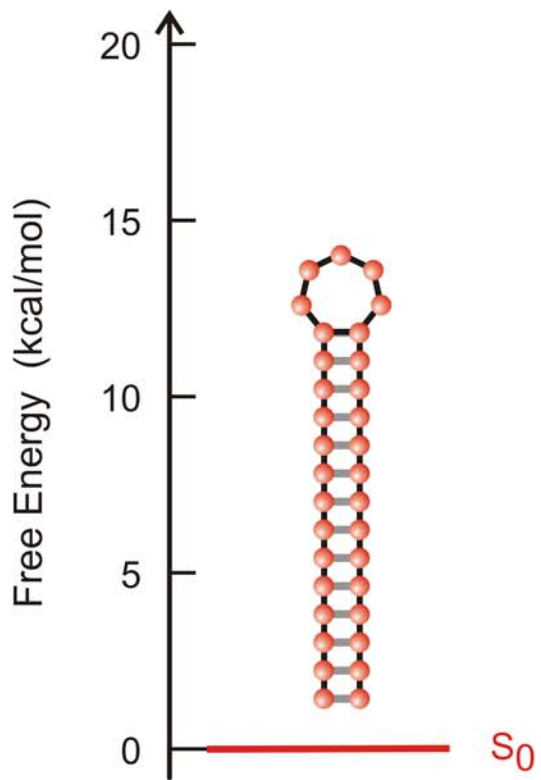


Reliability of structure prediction in tRNA^{phe}



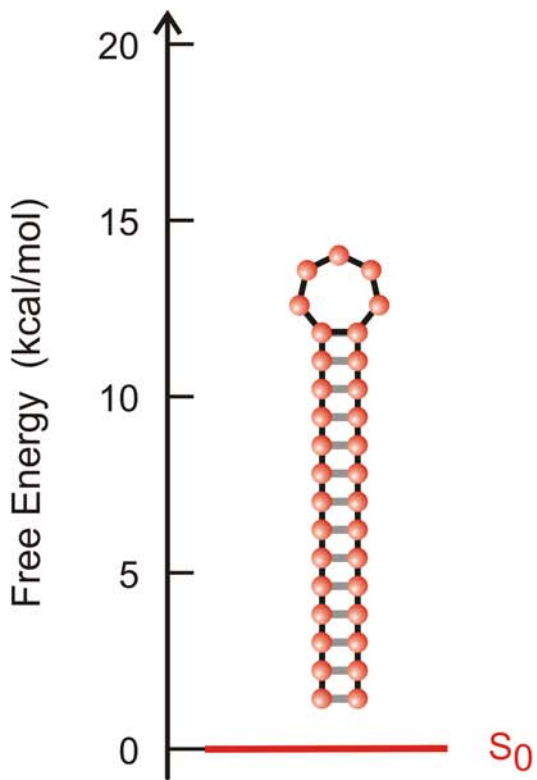
Reliability of structure prediction in 5S ribosomal RNA

One sequence - one structure



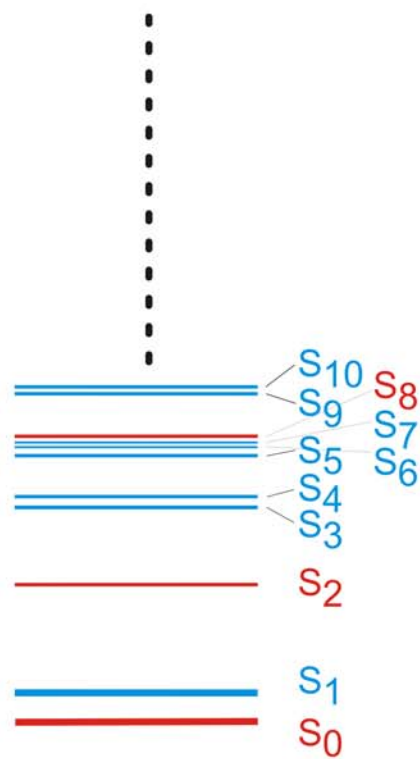
Minimum free energy structure

One sequence - one structure



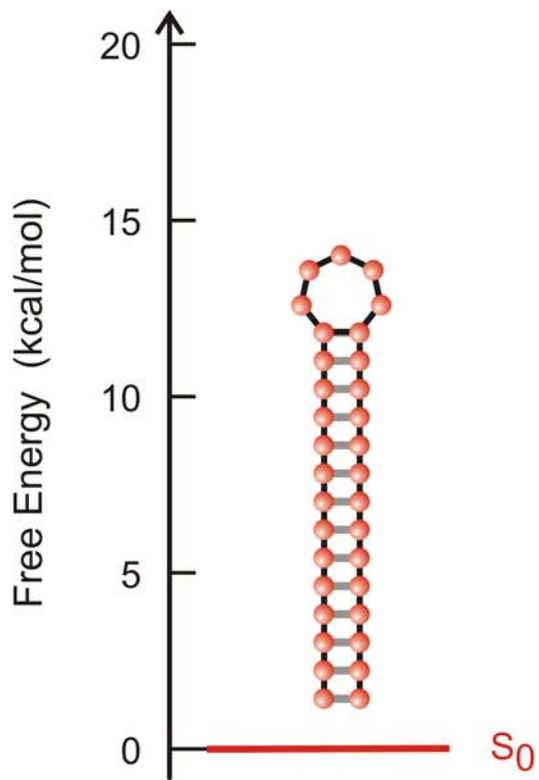
Minimum free energy structure

Many suboptimal structures
Partition function



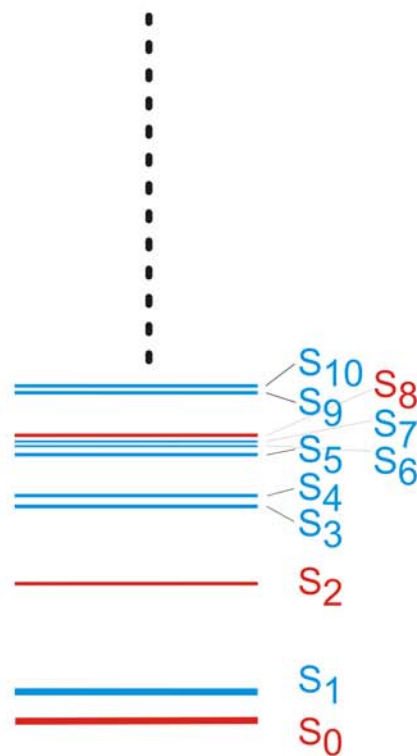
Suboptimal structures

One sequence - one structure



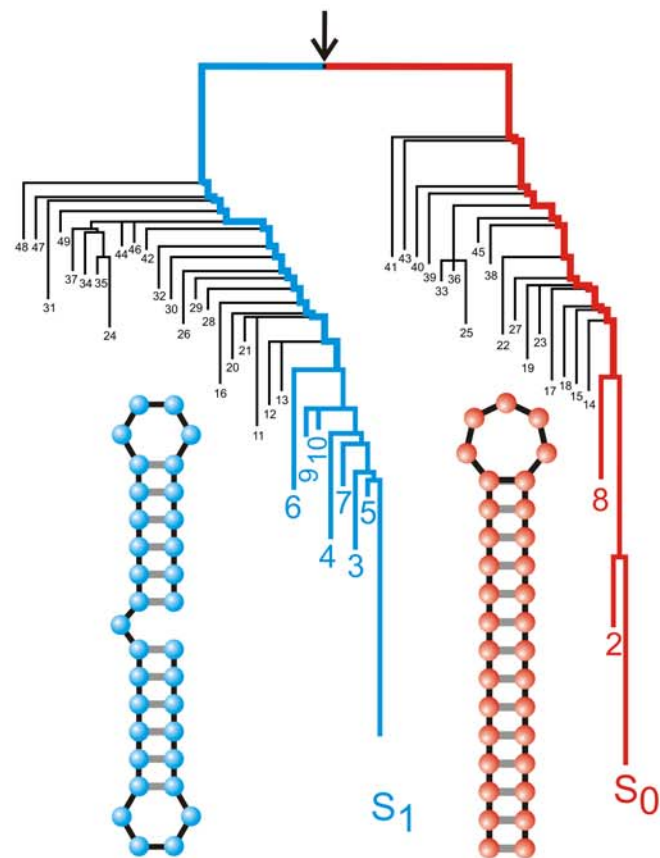
Minimum free energy structure

Many suboptimal structures
Partition function



Suboptimal structures

Metastable structures
Conformational switches



Kinetic structures

The Folding Algorithm

A sequence \mathbf{I} specifies an energy ordered set of compatible structures $\mathfrak{S}(\mathbf{I})$:

$$\mathfrak{S}(\mathbf{I}) = \{\mathbf{S}_0, \mathbf{S}_1, \dots, \mathbf{S}_m, \mathbf{O}\}$$

A trajectory $\mathfrak{Z}_k(\mathbf{I})$ is a time ordered series of structures in $\mathfrak{S}(\mathbf{I})$. A folding trajectory is defined by starting with the open chain \mathbf{O} and ending with the global minimum free energy structure \mathbf{S}_0 or a metastable structure \mathbf{S}_k which represents a local energy minimum:

$$\mathfrak{Z}_0(\mathbf{I}) = \{\mathbf{O}, \mathbf{S}(1), \dots, \mathbf{S}(t-1), \mathbf{S}(t), \mathbf{S}(t+1), \dots, \mathbf{S}_0\}$$

$$\mathfrak{Z}_k(\mathbf{I}) = \{\mathbf{O}, \mathbf{S}(1), \dots, \mathbf{S}(t-1), \mathbf{S}(t), \mathbf{S}(t+1), \dots, \mathbf{S}_k\}$$

Formulation of kinetic RNA folding as a stochastic process

Master equation

$$\frac{dP_k}{dt} = \sum_{i=0}^{m+1} (P_{ik}(t) - P_{ki}(t)) = \sum_{i=0}^{m+1} k_{ik} P_i - P_k \sum_{i=0}^{m+1} k_{ki}$$

$$k = 0, 1, \dots, m+1$$

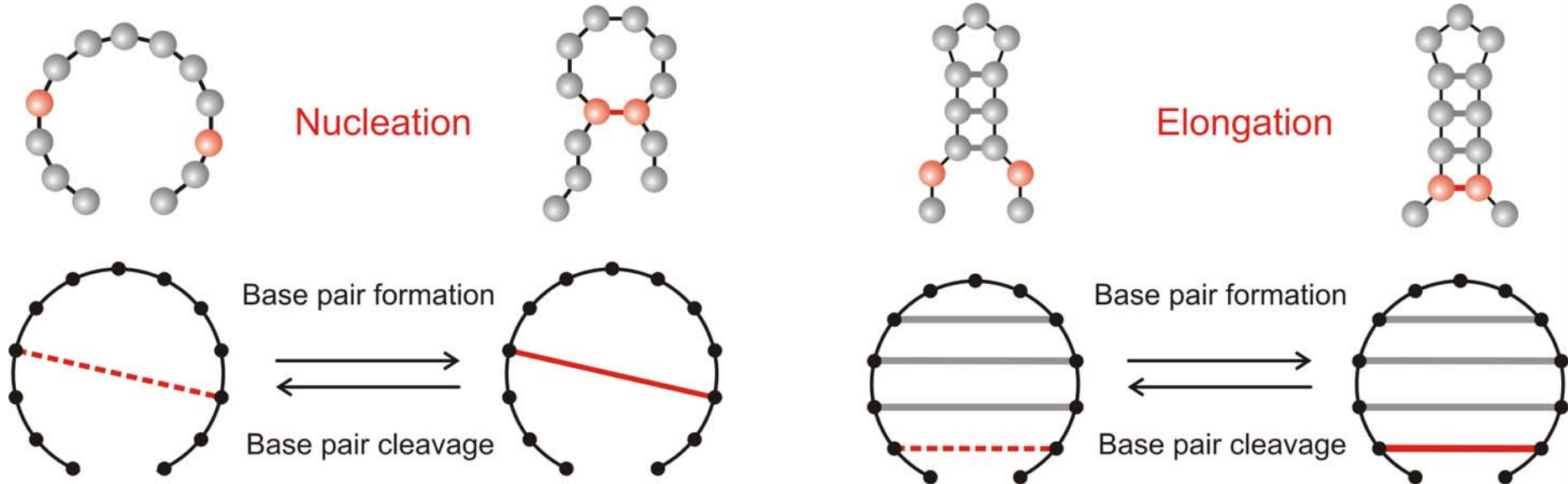
Transition probabilities $P_{ij}(t) = \text{Prob}\{\mathbf{S}_i \rightarrow \mathbf{S}_j\}$ are defined by

$$P_{ij}(t) = P_i(t) k_{ij} = P_i(t) \exp(-\Delta G_{ij}/2RT) / \Sigma_i$$

$$P_{ji}(t) = P_j(t) k_{ji} = P_j(t) \exp(-\Delta G_{ji}/2RT) / \Sigma_j$$

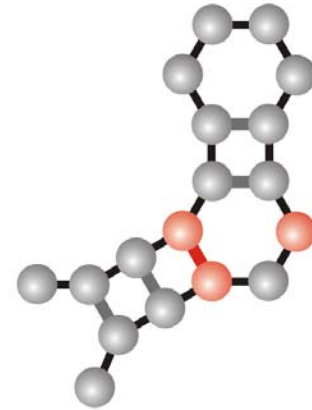
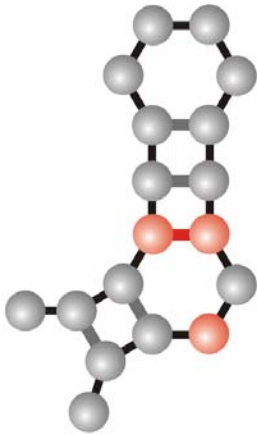
$$\Sigma_k = \sum_{k=1, k \neq i}^{m+2} \exp(-\Delta G_{ki}/2RT)$$

The symmetric rule for transition rate parameters is due to Kawasaki (K. Kawasaki, *Diffusion constants near the critical point for time dependent Ising models*. Phys.Rev. **145**:224-230, 1966).



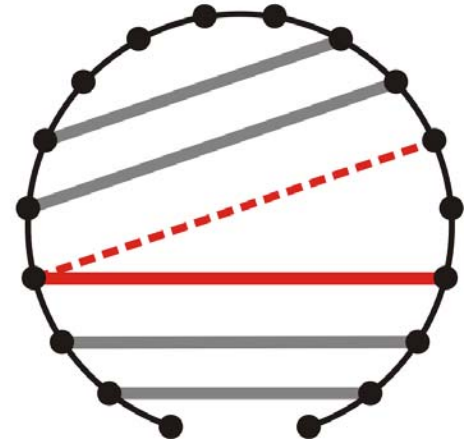
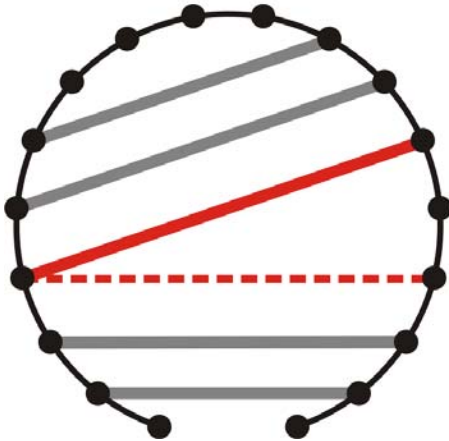
Corresponds to base pair distance: $d_p(S_1, S_2)$

Base pair formation and base pair cleavage moves for nucleation and elongation of stacks



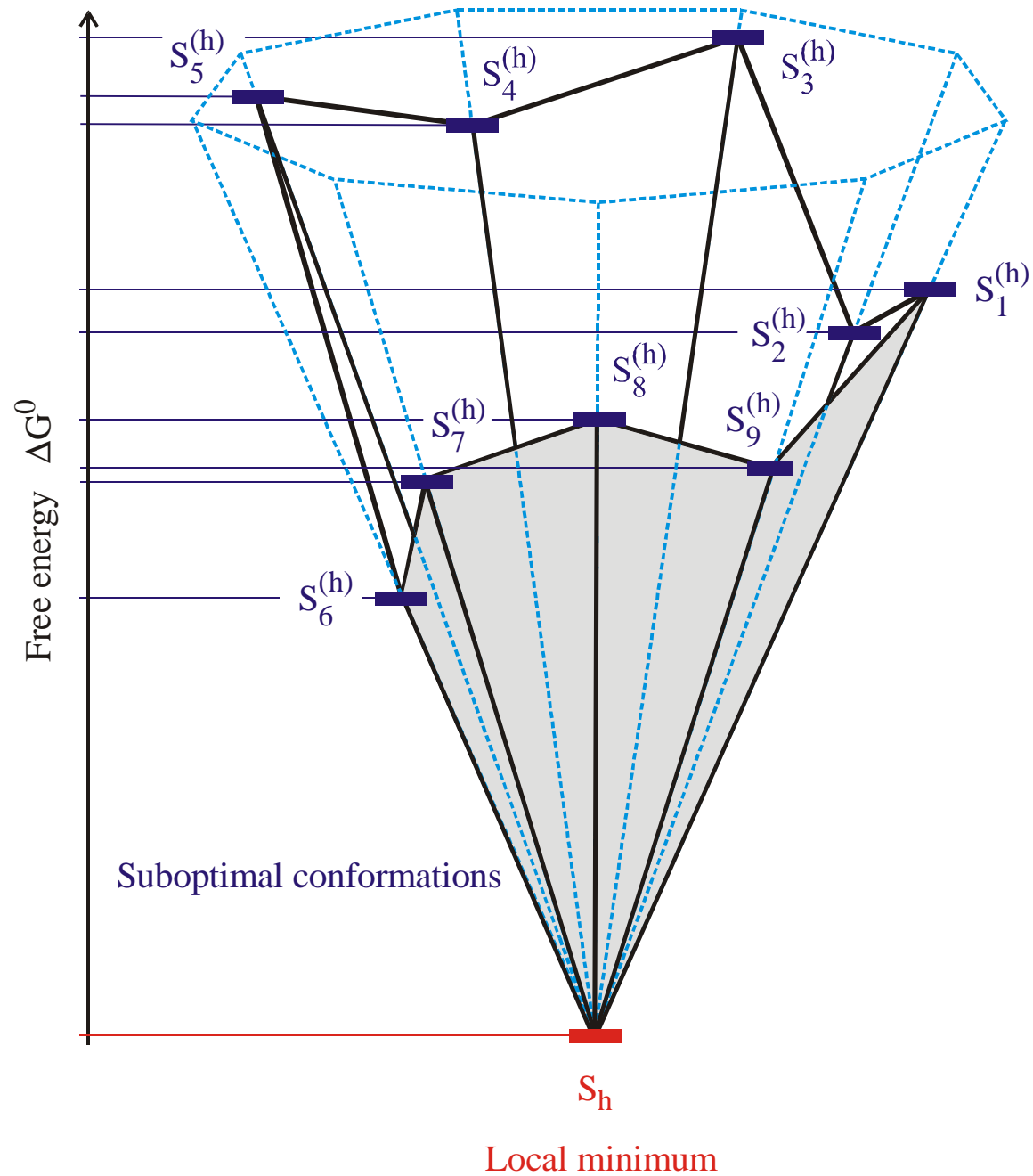
Base pair shift

Class 1

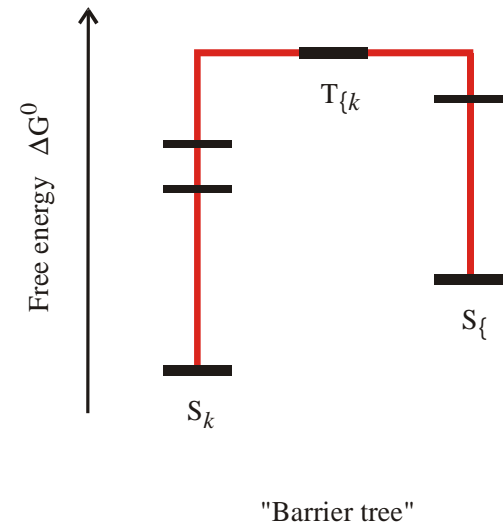
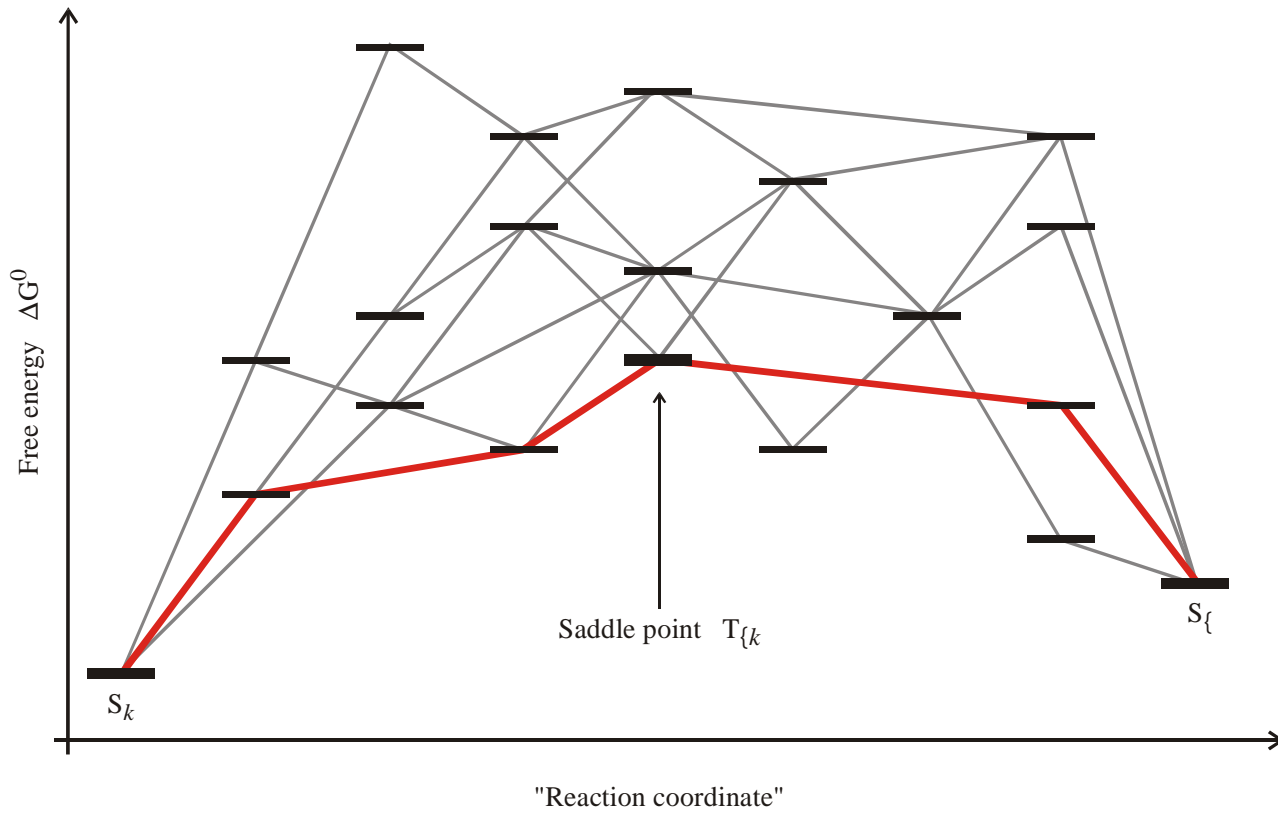


Base pair closure, opening and shift corresponds to Hamming distance: $d_H(S_1, S_2)$

Base pair shift move of class 1: Shift inside internal loops or bulges



Search for local minima in conformation space



Definition of a ,barrier tree‘

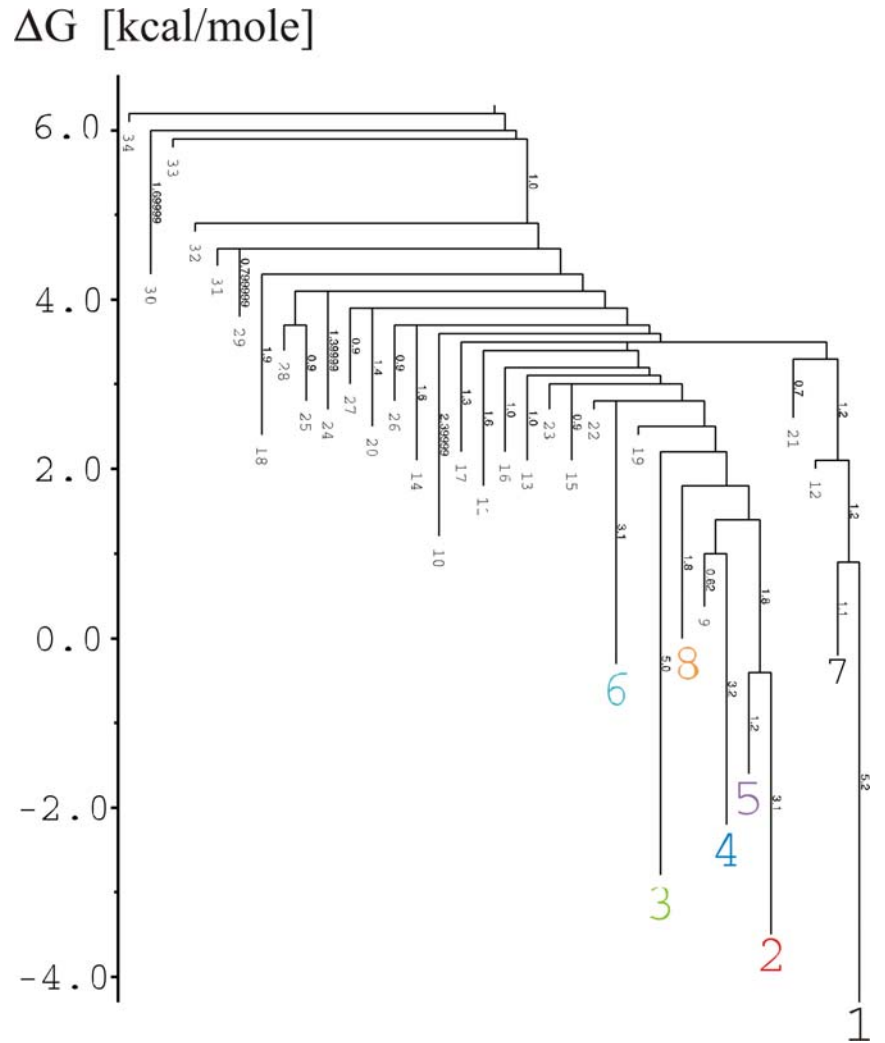
CUGCGGCUUUGGCUCUAGCC

.....((((.....)))))	-4.30
(((.....)).....)	-3.50
((.....)).....	-3.10
.....(((.....)))	-2.80
.....(((.....)))	-2.20
.....(((.....)))	-2.20
((.....)).....	-2.00
.....(((.....)))	-1.60
.....(((.....)))	-1.60
.....(((.....)))	-1.50
.....(((.....)))	-1.40
.....(((.....)))	-1.40
.....(((.....)))	-1.00
.....(((.....)))	-0.90
.....(((.....)))	-0.90
.....(((.....)))	-0.80
.....(((.....)))	-0.80
.....(((.....)))	-0.60
.....(((.....)))	-0.60
.....(((.....)))	-0.50
.....(((.....)))	-0.50
.....(((.....)))	-0.40
.....(((.....)))	-0.30
.....(((.....)))	-0.30
.....(((.....)))	-0.20
.....(((.....)))	-0.20
.....(((.....)))	-0.20
.....(((.....)))	0.00
.....(((.....)))	0.00
.....(((.....)))	0.10



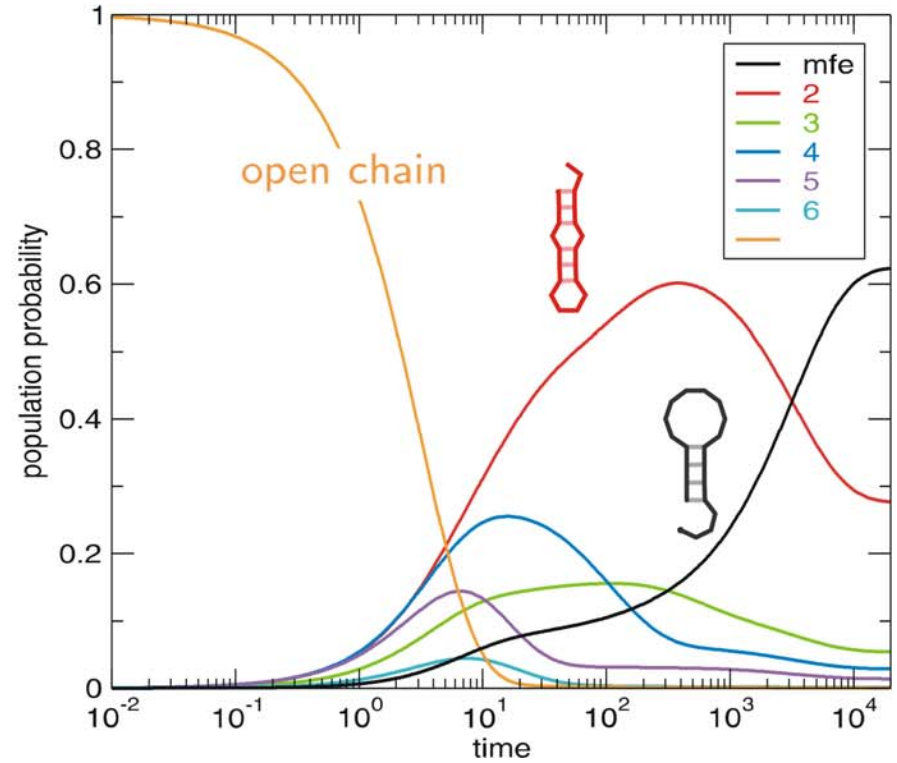
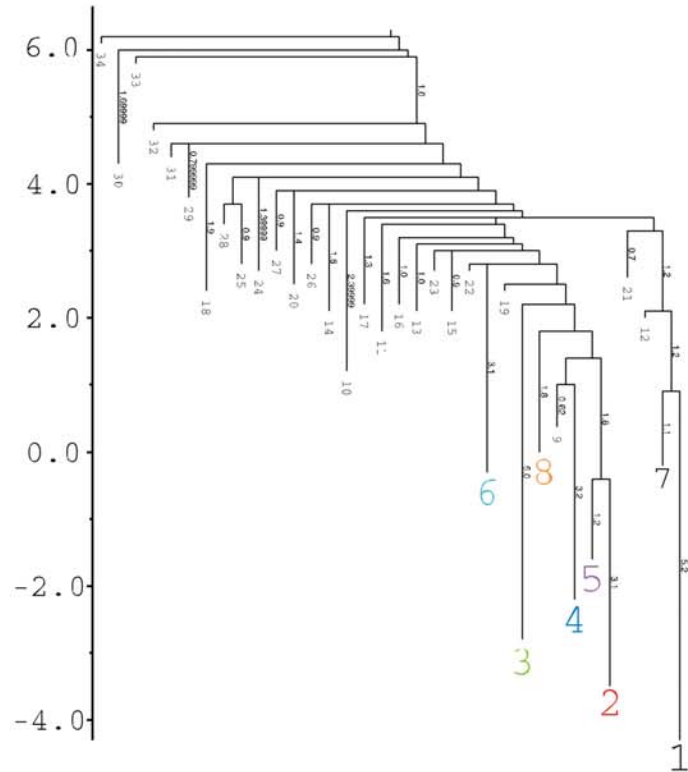
M.T. Wolfinger, W.A. Svrcek-Seiler, C. Flamm,
I.L. Hofacker, P.F. Stadler. 2004. *J.Phys.A:*
Math.Gen. **37**:4731-4741.

CUGCGGCUUUGGCUCUAGCC	
.....((((.....)))))	-4.30
(((.....)).....))..	-3.50
((.....)).....)	-3.10
.....(((.....)))	-2.80
.....((((.....)).....)	-2.20
.....((((.....)).....)	-2.20
((.....)).....)	-2.00
.....((((.....)).....)	-1.60
.....((((.....)).....)	-1.50
.....((((.....)).....)	-1.40
.....((((.....)).....)	-1.40
.....((((.....)).....)	-1.00
.....((((.....)).....)	-0.90
.....((((.....)).....)	-0.90
.....((((.....)).....)	-0.80
.....((((.....)).....)	-0.80
.....((((.....)).....)	-0.60
.....((((.....)).....)	-0.60
.....((((.....)).....)	-0.50
.....((((.....)).....)	-0.50
.....((((.....)).....)	-0.40
.....((((.....)).....)	-0.30
.....((((.....)).....)	-0.30
.....((((.....)).....)	-0.20
.....((((.....)).....)	-0.20
.....((((.....)).....)	0.00
.....((((.....)).....)	0.00
.....((((.....)).....)	0.10



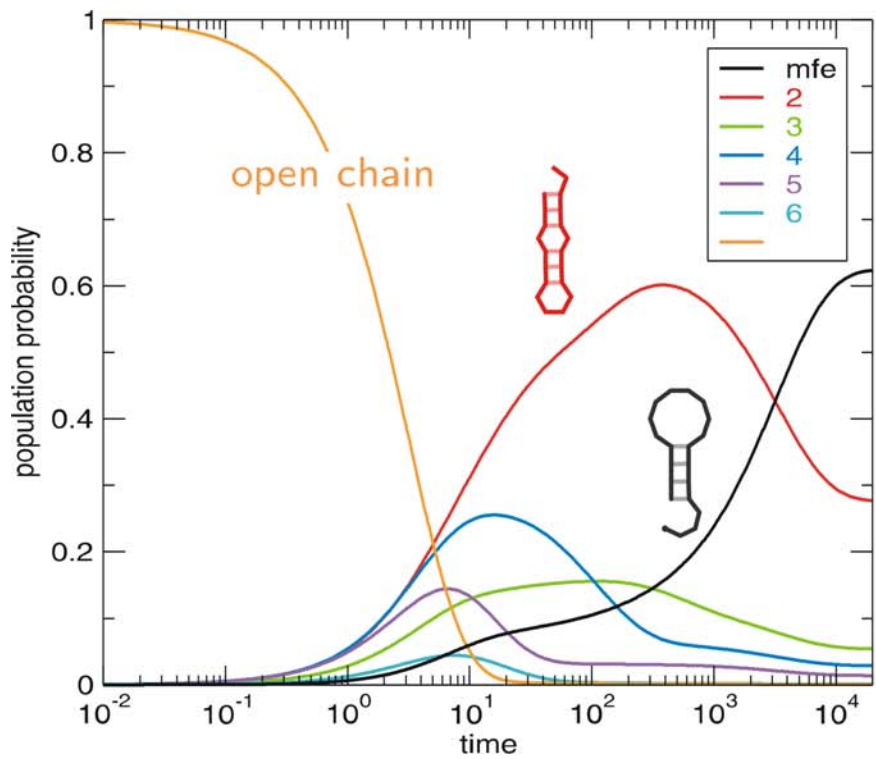
M.T. Wolfinger, W.A. Svrcek-Seiler, C. Flamm, I.L. Hofacker, P.F. Stadler. 2004. *J.Phys.A: Math.Gen.* **37**:4731-4741.

ΔG [kcal/mole]

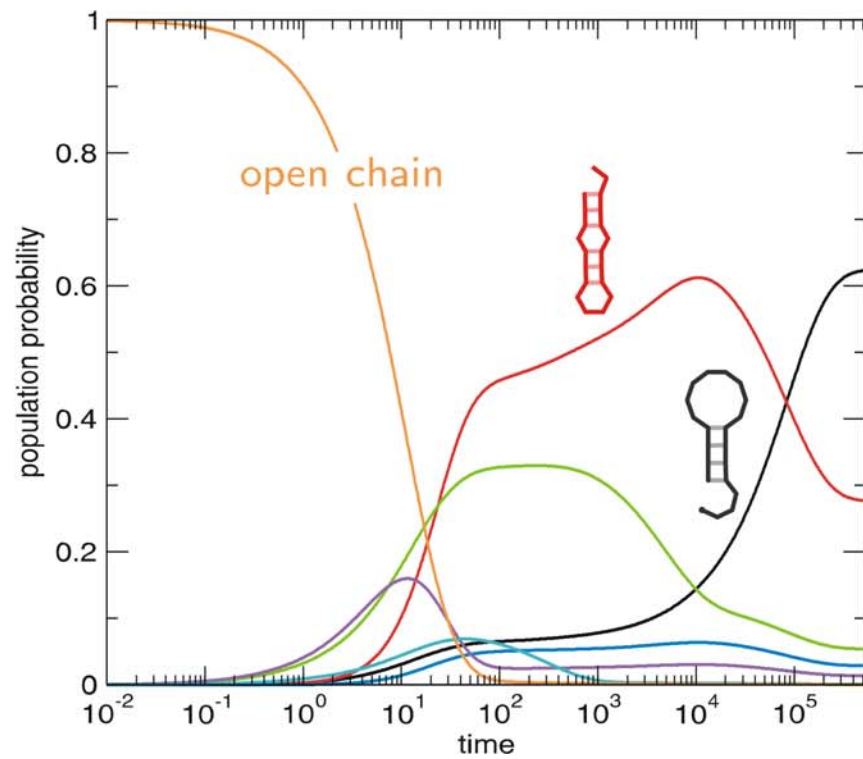


Arrhenius kinetics

M.T. Wolfinger, W.A. Svrcek-Seiler, C. Flamm,
I.L. Hofacker, P.F. Stadler. 2004. *J.Phys.A:*
Math.Gen. **37**:4731-4741.

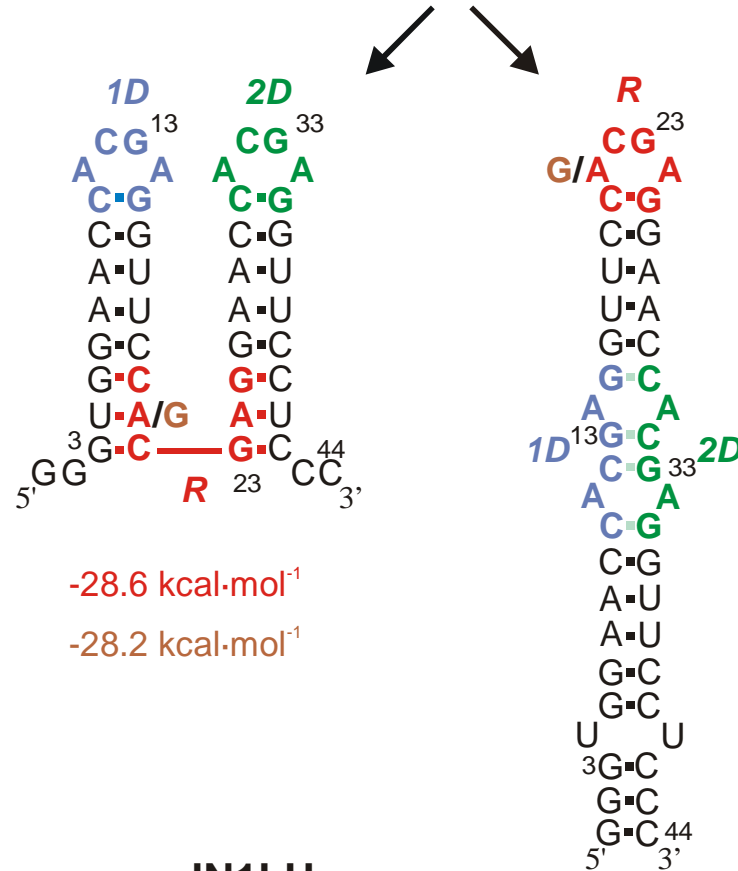


Arrhenius kinetic



Exact solution of the master equation

M.T. Wolfinger, W.A. Svrcek-Seiler, C. Flamm,
 I.L. Hofacker, P.F. Stadler. 2004. *J.Phys.A:*
Math.Gen. **37**:4731-4741.



-28.6 kcal·mol⁻¹

-28.2 kcal·mol⁻¹

-28.6 kcal·mol⁻¹

-31.8 kcal·mol⁻¹

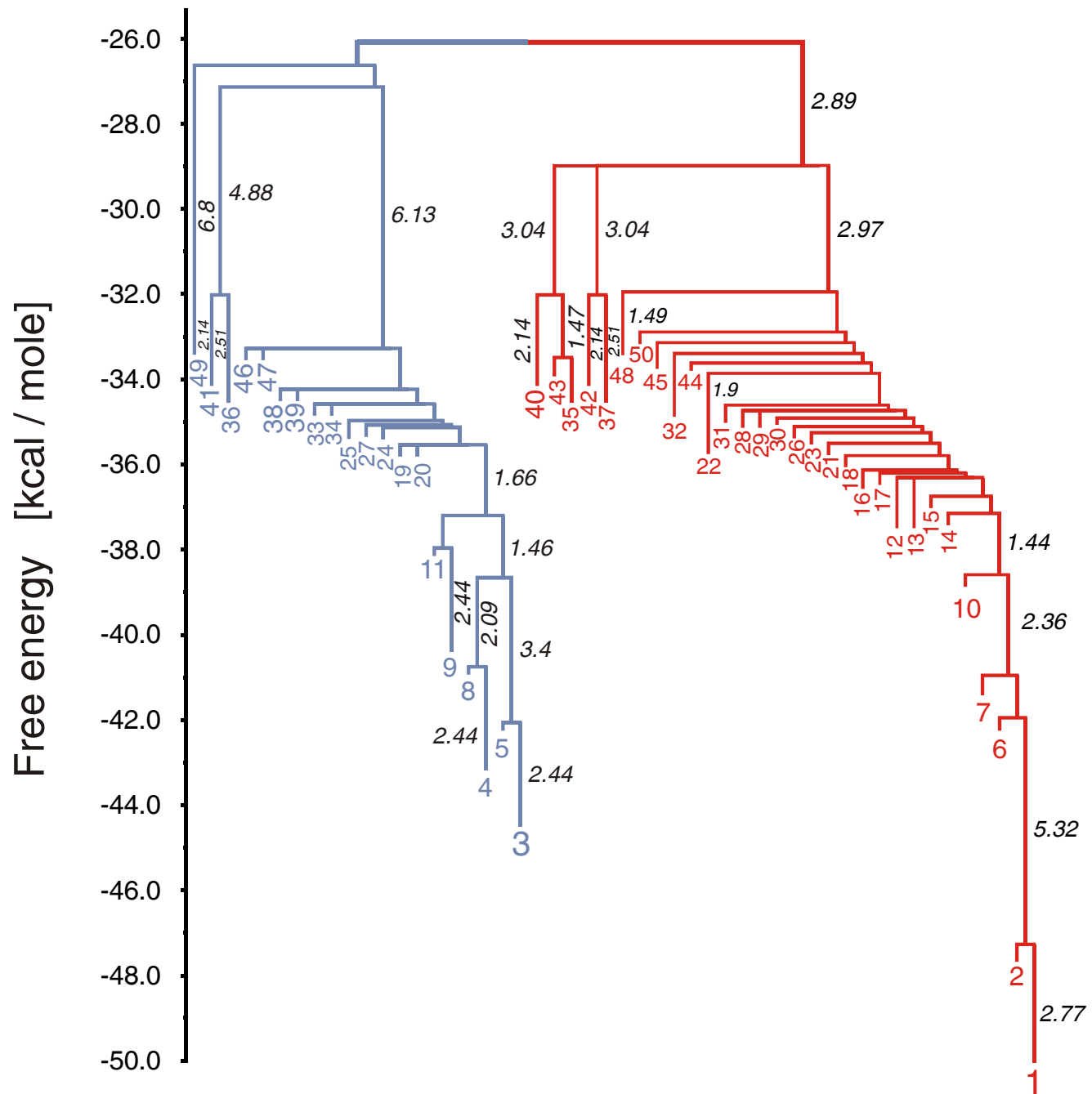
An RNA switch

JN1LH

J.H.A. Nagel, C. Flamm, I.L. Hofacker, K. Franke,
 M.H. de Smit, P. Schuster, and C.W.A. Pleij.

Structural parameters affecting the kinetic competition of
 RNA hairpin formation, *Nucleic Acids Res.*, in press 2006.

J1LH barrier tree



- minus the background levels observed in the HSP in the control (Sar1-GDP-containing) incubation that prevents COPII vesicle formation. In the microsome control, the level of p115-SNARE associations was less than 0.1%.
46. C. M. Carr, E. Grote, M. Munson, F. M. Hughson, P. J. Novick, *J. Cell Biol.* **146**, 333 (1999).
 47. C. Ungermann, B. J. Nichols, H. R. Pelham, W. Wickner, *J. Cell Biol.* **140**, 61 (1998).
 48. E. Grote and P. J. Novick, *Mol. Biol. Cell* **10**, 4149 (1999).
 49. P. Uetz et al., *Nature* **403**, 623 (2000).
 50. GST-SNARE proteins were expressed in bacteria and purified on glutathione-Sepharose beads using standard methods. Immobilized GST-SNARE protein (0.5 μ M) was incubated with rat liver cytosol (20 mg) or purified recombinant p115 (0.5 μ M) in 1 ml of NS buffer containing 1% BSA for 2 hours at 4°C with rotation. Beads were briefly spun (3000 rpm for 10 s) and sequentially washed three times with NS buffer and three times with NS buffer supplemented with 150 mM NaCl. Bound proteins were eluted three times in 50 μ l of 50 mM tris-HCl (pH 8.5), 50 mM reduced glutathione, 150 mM NaCl, and 0.1% Triton X-100 for 15 min at 4°C with intermittent mixing, and elutes were pooled. Proteins were precipitated by MeOH/CH₂Cl₂ and separated by SDS-polyacrylamide gel electrophoresis (PAGE) followed by immunoblotting using p115 mAb 13F12.
 51. V. Rybin et al., *Nature* **383**, 266 (1996).
 52. K. G. Hardwick and H. R. Pelham, *J. Cell Biol.* **119**, 513 (1992).
 53. A. P. Newman, M. E. Groesch, S. Ferro-Novick, *EMBO J.* **11**, 3609 (1992).
 54. A. Spang and R. Schekman, *J. Cell Biol.* **143**, 589 (1998).
 55. M. F. Rexach, M. Latterich, R. W. Schekman, *J. Cell Biol.* **126**, 1133 (1994).
 56. A. Mayer and W. Wickner, *J. Cell Biol.* **136**, 307 (1997).
 57. M. D. Turner, H. Plutner, W. E. Balch, *J. Biol. Chem.* **272**, 13479 (1997).
 58. A. Price, D. Seals, W. Wickner, C. Ungermann, *J. Cell Biol.* **148**, 1231 (2000).
 59. X. Cao and C. Barlowe, *J. Cell Biol.* **149**, 55 (2000).
 60. G. G. Tall, H. Hama, D. B. DeWald, B. F. Horadzovsky, *Mol. Biol. Cell* **10**, 1873 (1999).
 61. C. G. Burd, M. Peterson, C. R. Cowles, S. D. Emr, *Mol. Biol. Cell* **8**, 1089 (1997).
 62. M. R. Peterson, C. G. Burd, S. D. Emr, *Curr. Biol.* **9**, 159 (1999).
 63. M. G. Waters, D. O. Clary, J. E. Rothman, *J. Cell Biol.* **118**, 1015 (1992).
 64. D. M. Walter, K. S. Paul, M. G. Waters, *J. Biol. Chem.* **273**, 29565 (1998).
 65. N. Hui et al., *Mol. Biol. Cell* **8**, 1777 (1997).
 66. T. E. Kreis, *EMBO J.* **5**, 931 (1986).
 67. H. Plutner, H. W. Davidson, J. Saraste, W. E. Balch, *J. Cell Biol.* **119**, 1097 (1992).
 68. D. S. Nelson et al., *J. Cell Biol.* **143**, 319 (1998).
 69. We thank G. Waters for p115 cDNA and p115 mAbs; G. Warren for p97 and p47 antibodies; R. Scheller for rbt1, membrin, and sec22 cDNAs; H. Plutner for excellent technical assistance; and P. Tan for help during the initial phase of this work. Supported by NIH grants GM 33301 and GM42336 and National Cancer Institute grant CA58689 (W.E.B.), a NIH National Research Service Award (B.D.M.), and a Wellcome Trust International Traveling Fellowship (B.B.A.).

20 March 2000; accepted 22 May 2000

One Sequence, Two Ribozymes: Implications for the Emergence of New Ribozyme Folds

Erik A. Schultes and David P. Bartel*

We describe a single RNA sequence that can assume either of two ribozyme folds and catalyze the two respective reactions. The two ribozyme folds share no evolutionary history and are completely different, with no base pairs (and probably no hydrogen bonds) in common. Minor variants of this sequence are highly active for one or the other reaction, and can be accessed from prototype ribozymes through a series of neutral mutations. Thus, in the course of evolution, new RNA folds could arise from preexisting folds, without the need to carry inactive intermediate sequences. This raises the possibility that biological RNAs having no structural or functional similarity might share a common ancestry. Furthermore, functional and structural divergence might, in some cases, precede rather than follow gene duplication.

Related protein or RNA sequences with the same folded conformation can often perform very different biochemical functions, indicating that new biochemical functions can arise from preexisting folds. But what evolutionary mechanisms give rise to sequences with new macromolecular folds? When considering the origin of new folds, it is useful to picture, among all sequence possibilities, the distribution of sequences with a particular fold and function. This distribution can range very far in sequence space (1). For example, only seven nucleotides are strictly conserved among the group I self-splicing introns, yet secondary (and presumably tertiary) structure within the core of the ribozyme is preserved (2). Because these dis-

parate isolates have the same fold and function, it is thought that they descended from a common ancestor through a series of mutational variants that were each functional. Hence, sequence heterogeneity among divergent isolates implies the existence of paths through sequence space that have allowed neutral drift from the ancestral sequence to each isolate. The set of all possible neutral paths composes a "neutral network," connecting in sequence space those widely dispersed sequences sharing a particular fold and activity, such that any sequence on the network can potentially access very distant sequences by neutral mutations (3-5).

Theoretical analyses using algorithms for predicting RNA secondary structure have suggested that different neutral networks are interwoven and can approach each other very closely (3, 5-8). Of particular interest is whether ribozyme neutral networks approach each other so closely that they intersect. If so, a single sequence would be capable of folding into two different conformations, would

have two different catalytic activities, and could access by neutral drift every sequence on both networks. With intersecting networks, RNAs with novel structures and activities could arise from previously existing ribozymes, without the need to carry non-functional sequences as evolutionary intermediates. Here, we explore the proximity of neutral networks experimentally, at the level of RNA function. We describe a close apposition of the neutral networks for the hepatitis delta virus (HDV) self-cleaving ribozyme and the class III self-ligating ribozyme.

In choosing the two ribozymes for this investigation, an important criterion was that they share no evolutionary history that might confound the evolutionary interpretations of our results. Choosing at least one artificial ribozyme ensured independent evolutionary histories. The class III ligase is a synthetic ribozyme isolated previously from a pool of random RNA sequences (9). It joins an oligonucleotide substrate to its 5' terminus. The prototype ligase sequence (Fig. 1A) is a shortened version of the most active class III variant isolated after 10 cycles of *in vitro* selection and evolution. This minimal construct retains the activity of the full-length isolate (10). The HDV ribozyme carries out the site-specific self-cleavage reactions needed during the life cycle of HDV, a satellite virus of hepatitis B with a circular, single-stranded RNA genome (11). The prototype HDV construct for our study (Fig. 1B) is a shortened version of the antigenomic HDV ribozyme (12), which undergoes self-cleavage at a rate similar to that reported for other antigenomic constructs (13, 14).

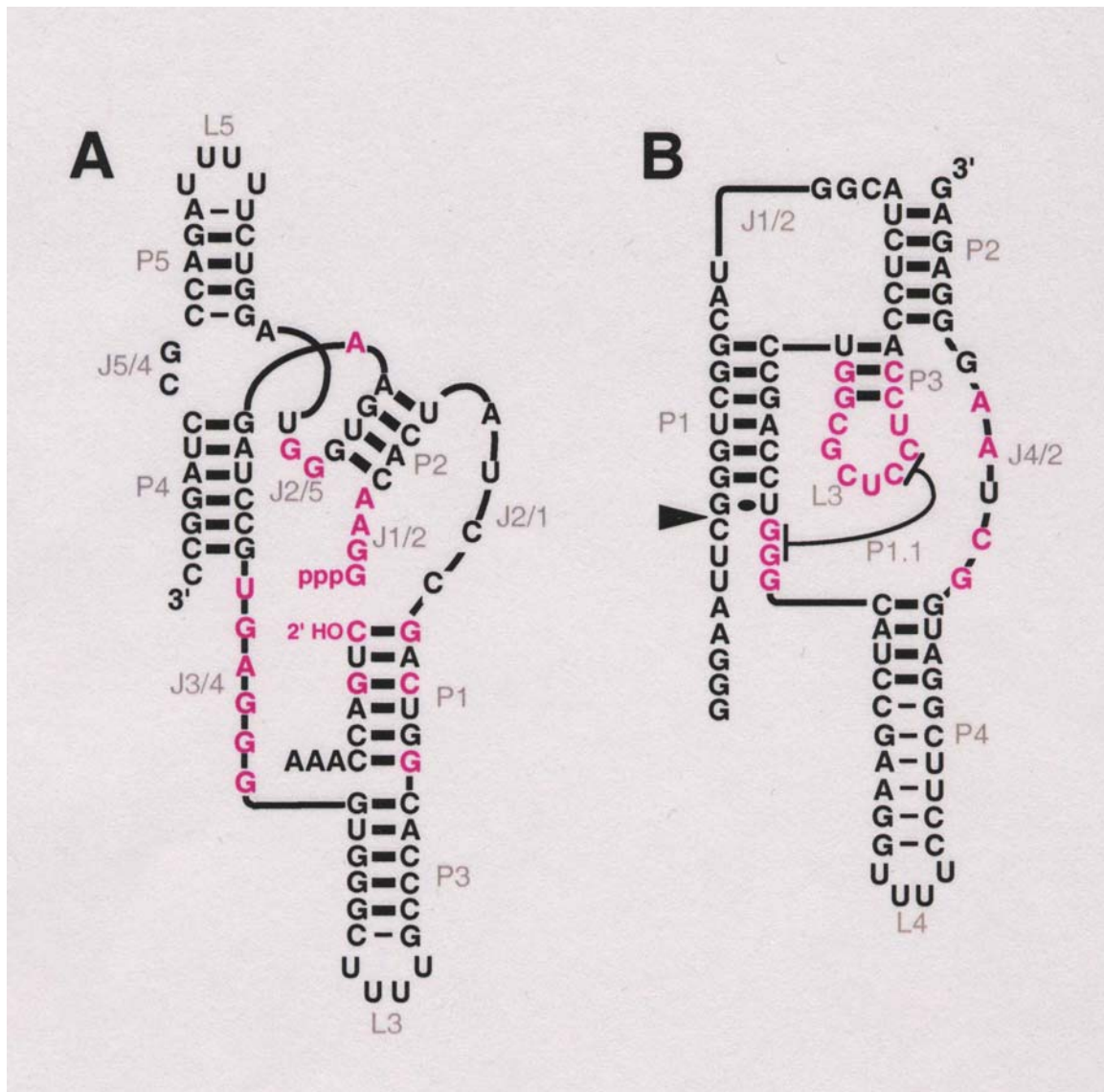
The prototype class III and HDV ribozymes have no more than the 25% sequence identity expected by chance and no fortuitous structural similarities that might favor an intersection of their two neutral networks. Nevertheless, sequences can be designed that simultaneously satisfy the base-pairing requirements

A ribozyme switch

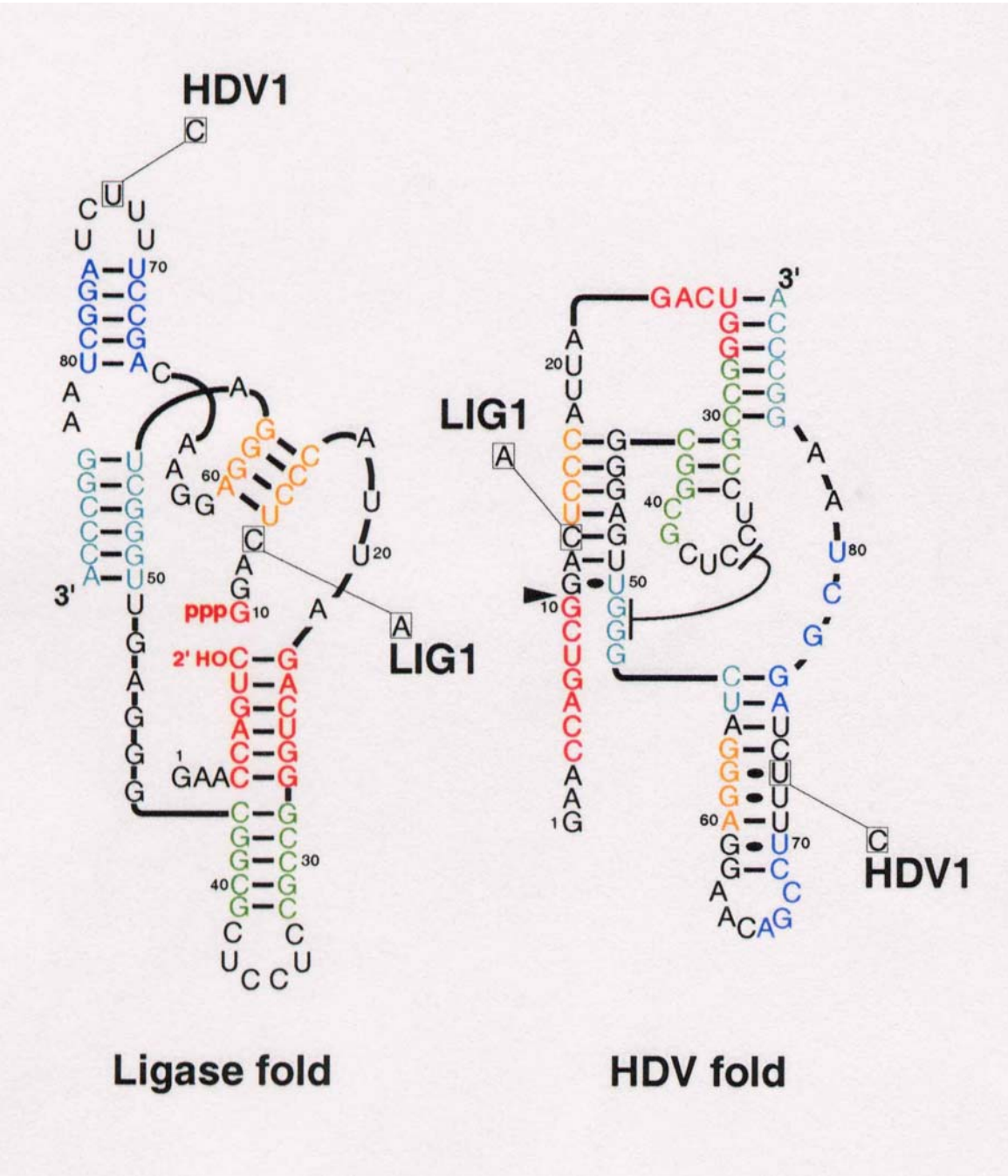
E.A.Schultes, D.B.Bartel, *Science*
289 (2000), 448-452

Whitehead Institute for Biomedical Research and Department of Biology, Massachusetts Institute of Technology, 9 Cambridge Center, Cambridge, MA 02142, USA.

*To whom correspondence should be addressed. E-mail: dbartel@wi.mit.edu

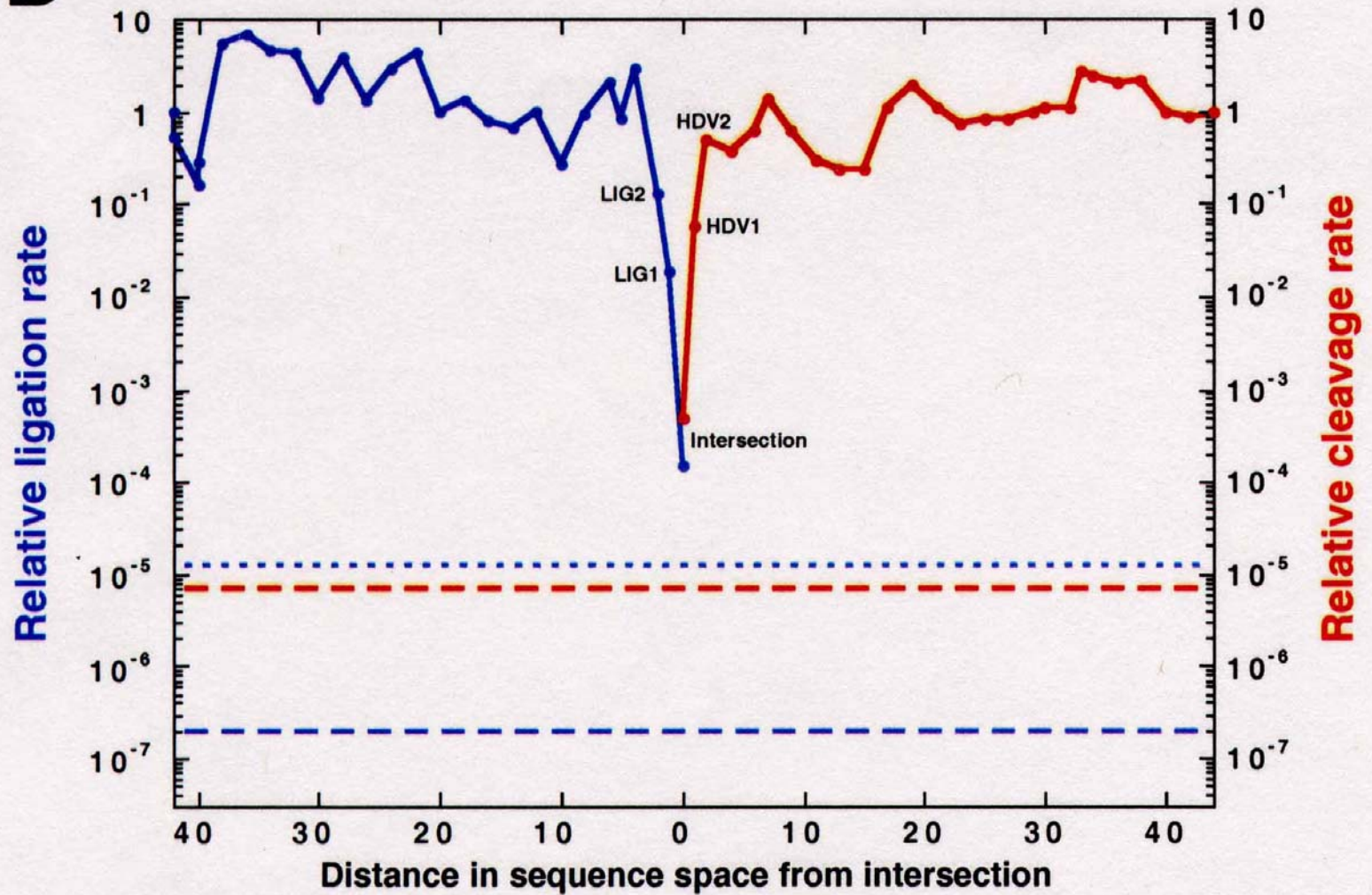


Two ribozymes of chain lengths $n = 88$ nucleotides: An artificial ligase (A) and a natural cleavage ribozyme of hepatitis- δ -virus (B)



The sequence at the *intersection*:

An RNA molecules which is 88 nucleotides long and can form both structures

B

Two neutral walks through sequence space with conservation of structure and catalytic activity

Acknowledgement of support

Fonds zur Förderung der wissenschaftlichen Forschung (FWF)
Projects No. 09942, 10578, 11065, 13093
13887, and 14898

Wiener Wissenschafts-, Forschungs- und Technologiefonds (WWTF)
Project No. Mat05

Jubiläumsfonds der Österreichischen Nationalbank
Project No. Nat-7813

European Commission: Contracts No. 98-0189, 12835 (NEST)

Austrian Genome Research Program – GEN-AU: Bioinformatics
Network (BIN)

Österreichische Akademie der Wissenschaften

Siemens AG, Austria

Universität Wien and the Santa Fe Institute



Universität Wien

Coworkers

Peter Stadler, Bärbel M. Stadler, Universität Leipzig, GE

Paul E. Phillipson, University of Colorado at Boulder, CO

Heinz Engl, Philipp Kügler, James Lu, Stefan Müller, RICAM Linz, AT

Jord Nagel, Kees Pleij, Universiteit Leiden, NL

Walter Fontana, Harvard Medical School, MA

Christian Reidys, Christian Forst, Los Alamos National Laboratory, NM

Ulrike Göbel, Walter Grüner, Stefan Kopp, Jaqueline Weber, Institut für
Molekulare Biotechnologie, Jena, GE

Ivo L.Hofacker, Christoph Flamm, Andreas Svrček-Seiler, Universität Wien, AT

**Kurt Grünberger, Michael Kospach, Andreas Wernitznig, Stefanie Widder,
Stefan Wuchty, Andreas De Stefani**, Universität Wien, AT

**Jan Cupal, Stefan Bernhart, Lukas Endler, Ulrike Langhammer, Rainer Machne,
Ulrike Mückstein, Hakim Tafer, Thomas Taylor**, Universität Wien, AT



Universität Wien

Web-Page for further information:

<http://www.tbi.univie.ac.at/~pks>

